Thermal and Morphological Study of Segmented Multiblock Copolyesters Containing 2,2,4,4-Tetramethyl-1,3-cyclobutanediol

Ninad Dixit

Thesis submitted to the faculty of the Virginia Polytechnic Institute and State University in partial fulfillment of the requirements for the degree of

Master of Science

In

Chemistry

Robert B. Moore, Chair

Timothy E. Long

Herve Marand

S. Richard Turner

04/16/2012

Blacksburg, VA

Keywords: segmented block copolyester, morphology, differential scanning calorimetry, small angle X—ray scattering, glass transition, microphase separation

Thermal and Morphological Study of Segmented Multiblock Copolyesters Containing 2,2,4,4-Tetramethyl-1,3-cyclobutanediol

Ninad Dixit

ABSTRACT

Thermal and morphological studies of the segmented multiblock copolyesters containing 2,2,4,4-tetramethyl-1,3-cyclobutanediol and dimethyl-1,4-cyclohexane dicarboxylate were carried out using differential scanning calorimetry, small angle X-ray scattering, wide angle X-ray diffraction and dynamic mechanical analysis. Molecular origins of the thermal transitions appearing in copolyesters were assigned by the copolyester analysis at different temperatures. The hard segments in copolyesters underwent short-range and long-range ordering (crystallization) during cooling or annealing above glass transition temperature, as concluded from thermal and wide angle X-ray diffraction analysis. Annealing process affected the ordering in hard segments and annealing temperatures of 160 °C and above led to increased microphase mixing. The small angle X-ray scattering studies confirmed the microphase separated morphology of copolyesters and supported the argument of increased microphase mixing in copolyesters annealed at higher temperatures. The amount of sulfonate containing co-monomer and its presence in either hard or soft microphase affected the morphology of the copolyesters. Introduction of the sulfonate groups led to increased microphase mixing in copolyesters as well as destruction of long-range order in the hard segments.

Acknowledgements

I would like to thank the U.S. Army Research Laboratory and the U.S. Army Research Office under the Army Materials Center of Excellence Program for their financial support. I sincerely thank Nancy Zhang for providing all the materials and for a number of discussions that helped me to carry out this study. Her intellectual input to this study is invaluable.

I am also very grateful to my advisor, Professor Robert Moore. This work would not have been possible without his guidance, encouragement and support. I sincerely thank you for showing tremendous patience with me during the tough times. I hope to gain as much knowledge as possible from you during my tenure as a graduate student. I would also like to thank the committee members – Professors Timothy Long, Herve´ Marand, S. Richard Turner and David Dillard (ex-member) for their encouragement and support.

Last but not the least; I would like to thank my colleagues in Moore research group with whom I have had a fantastic graduate student life. Every day spent with you all, in the lab or outside, helped me to keep my spirit alive. I would like to acknowledge Dr. Gilles Divoux for the advices pertaining to my professional life. He has also played a significant role in my understanding of the thermal analysis of polymers. I am very thankful to Mingqiang Zhang for carrying out SAXS measurements in VT and at the Argonne National Lab. Scott Forbey became a dear friend over the last couple of years and his cheerful attitude has led to a very joyful atmosphere in Hahn labs. I owe him many thanks for being a constant source of encouragement. Many thanks to other group members – Amanda, Jeremy, Elise, Katherine, Orkun, Xijing and Dr. Junbo Hou for being great colleagues and I look forward to be a part of this group in near future as well. Thank you all!

Table of Contents

List of Figures:

List of Tables:

Chapter 1: Thermal Analysis and Morphology of Segmented Multiblock Copolymers – A Literature Review

1.1 Introduction

Segmented multiblock copolymers are an important class of thermoplastic elastomers and have been applied in a variety of industries including coatings[1], packaging[2,3], adhesives.[4] These copolymers consist of short but large number of segments. Depending on the segment length and chemical structure of each segment, these copolymers may exhibit a microphase separated structure, which invokes their unique physical and mechanical properties.[5] Generally, one of the phases (i.e. soft microphase) is in a rubbery or viscous state while the other (i.e. hard microphase) is in a glassy or crystalline state. The hard microphase acts as a physical crosslink to the soft microphase. These crosslinks are thermally reversible, which greatly improve the processibility of segmented block copolymers.

There are several factors responsible for aggregation and microphase separation (i.e. domain formation) of the hard and soft segments. In the case of styrene-butadiene-styrene copolymers, the chemical incompatibility of the constituting monomers leads to microphase separation.[6] If the segments are crystallizable, such as polyesters, their crystallization will lead to microphase separation.[7] The strength and number of microphase separated domains in these copolymers dictates their performance at service temperature. For example, a crystalline hard microphase is likely to impart better mechanical properties than non-crystalline hard microphase at high temperature as crystalline domains would generally melt and flow at much higher temperature than the glass transition temperature of amorphous hard segments of the constituent polymer. Copolymers with greater hard segment content are likely to exhibit higher mechanical modulus at service temperature. Depending on the nature of the constituent segments and

processing conditions such as annealing, properties of segmented copolymers can range from that of elastomers to random copolymers. To achieve the properties of an elastomer, the segmented block copolymers are required to undergo significant microphase separation at service temperature. Microphase separation leads to development of specific morphological features, which affect the mechanical and other properties of the copolymer.

Increasing environmental safety concerns have driven researchers to focus on the synthesis of polymers in the absence of organic solvents as well as using monomers obtained from renewable resources.[8,9,10] Polyesters offer an excellent opportunity due to their melt condensation synthesis and monomers obtained from natural resources.[8,9] Additionally, the hydrolytic reactivity of polyesters provides a good post-consumer degradation mechanism.[11] Hence, an all-polyester segmented block copolymer could be a very significant step towards making environmentally friendly polymers. However, there is very limited literature available on segmented copolymers that contain polyester based hard and soft blocks. The ring opening polymerization of cyclic monomers (lactides and menthides) resulting in triblock copolymers has been described in literature.[12] However, ring opening methods limit the monomer selection, and residues of solvents used in the polymerization may not be suitable for biomedical applications. This study is focused on the morphological characterization of polyester-polyester copolymers synthesized via melt condensation. This is the first attempt towards understanding the morphology, thermal and mechanical properties of segmented multiblock copolyesters, which may lead to the identification of the interactions responsible for microphase separation in such systems.

This chapter briefly reviews analytical techniques used for the study of polyester-polyester copolymers, focusing on differential scanning calorimetry (DSC), small angle X-ray

scattering (SAXS) and dynamic mechanical analysis (DMA). Furthermore, the application of these techniques will be shown to offer an improved understanding of the morphology of segmented multiblock copolymers. Since this study includes segmented multiblock copolymers based on sulfonate containing hard and soft segments, ion containing segmented polyurethanes and polyester-ethers will also be discussed briefly.

1.2 Analytical Techniques for morphological analysis of segmented multiblock copolymers

1.2.1 Differential Scanning Calorimetry (DSC)

DSC is one of the most widely used techniques to characterize segmented block copolymers. The morphology of thermoplastic polyurethanes has been studied extensively by DSC and the amount of published literature provides a sound base for the characterization of other types of thermoplastic segmented block copolymers.[13] The instrument used to generate the reported data is a "heat flux" DSC. In this type of DSC, a sealed pan containing the sample, and an empty reference pan sit on a thermoelectric disc. The disc is located in a furnace and it transfers heat to the pans to keep their temperature identical. The differential between the heats provided to the sample and reference pans is recorded and used for further calculations of heat flow and heat capacity of samples.[14]

The following figure shows a typical DSC thermogram of thermoplastic segmented polyurethanes.

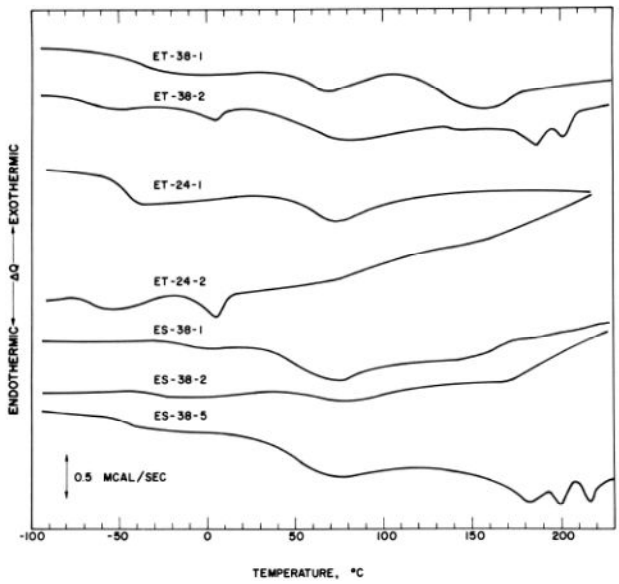

Figure 1.1: DSC thermograms of various polyurethanes based on MDI-BD hard segments and PTMO soft segments.[15] Reprinted with permission from *Multiphase Polymers*. AMERICAN CHEMICAL SOCIETY: 1979; Vol. 176, p 660. Copyright 1979 American Chemical Society.

The baseline shift observed in the temperature range of -60 ^{0}C to -10 ^{0}C corresponds to the glass transition in soft segments. Changes in the soft segment glass transition temperature (T_g) values have been used to estimate the degree of microphase mixing. For example, significant increase in soft segment T_g with increasing hard segment content in the elastomer indicates increased mixing of hard segments with the soft segments. If the soft segment T_g changes are not significant, the majority of the hard segments are present in the hard microphase only. Soft segment T_g depends on several other factors such as the molecular weight of the soft and hard segments, crystallization of either of the segments and solubility of soft and hard segments.[15]

Camberlin and Pascault[16] reported the quantitative analysis of microphase separation in polyurethanes by comparing the heat capacity changes of pure soft segments and those of

polyurethanes during the soft segment glass transition process. The extent of phase segregation was calculated using the following equation:

$$Phase\ segregation\ extent = \frac{\Delta C_{P2}}{\Delta C_{P1}} \quad (1)$$

Where, ΔC_{P1} is the heat capacity change for pure soft segments and ΔC_{P2} is the heat capacity change per gram of soft segment in the elastomer during the soft segment glass transition.

This analysis was based on the observation that the heat capacity change associated with the hard segment glass transition was negligible. For a relatively pure soft microphase, the soft segment glass transition is usually sharp. However, as more hard segments are mixed in with soft segments, the glass transition takes place over a broader temperature range. In addition, the concentration of soft segments decreases as more hard segments are mixed into the soft microphase. Hence, ΔC_P associated with the glass transition of soft segments (per unit mass of copolymer) decreases as well.

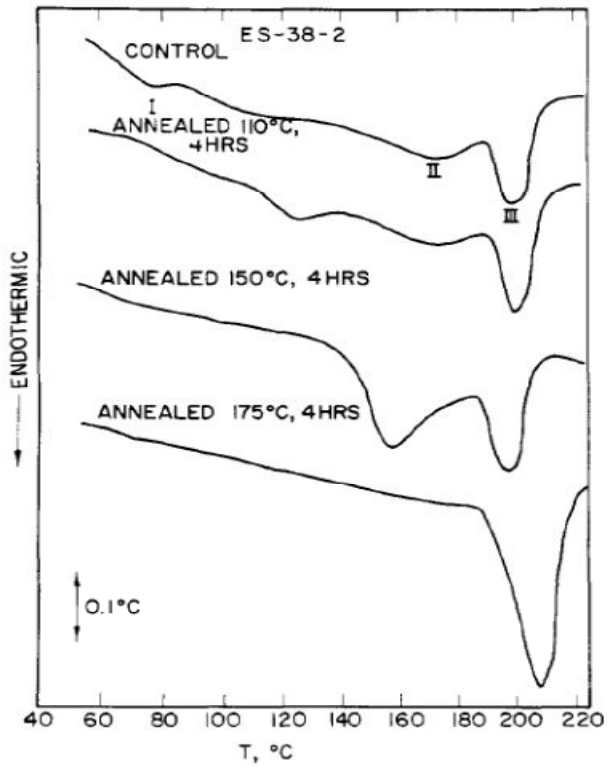

Figure 1.2: DSC thermograms of polyurethane based on MDI, butanediol and polybutylene adipate annealed at various temperatures.[17] Reprinted with permission from Seymour, R. W.; Cooper, S. L., Thermal Analysis of Polyurethane Block Polymers. *Macromolecules* **1973,** *6* (1), 48-53. Copyright 1973. American Chemical Society.

Generally, three types of endothermic transitions are observed as seen in Figure 1.2. Seymour et al.[17] reported that the peak centered around 70 °C (T_I) moved to higher temperatures with increasing annealing temperatures (in air, for 4 hours) and eventually merged with the peak centered at 160 °C (T_{II}). Annealing at even higher temperatures resulted in the merging of peaks centered at 160 ^{0}C and 185 ^{0}C (T_{III}). They also studied a range of compositions of polyurethanes synthesized using various isocyanates, some of which that could form hydrogen bonds, while others could not. They observed that the T_{II} transitions were independent of the extent of hydrogen bonding in hard segments. The DSC thermograms of polyurethanes with different hard segments (hydrogen bonding and non-hydrogen bonding) but similar weight percent compositions were very similar. Hesketh et al.[18] observed that the position of T_{III} was not

affected by annealing temperatures, suggesting a very regular arrangement of hard segments; i.e. crystallites, which exhibited a definite melting point. Castles et al.[19] studied copolyester-ethers wherein the hard segment consisted of poly(tetramethylene terephthalate) (PTMT) and poly(tetramethylene isophthalate) (PTMI). They observed that crystallinity and the melting point of hard segments decreased with increasing content of PTMI. Subsequently, a lower storage modulus was observed during dynamic mechanical analysis. Hence, they concluded that the dispersion of hard segment crystallites has a significant effect on the mechanical properties of copolyesters-ethers. Schick et al.[20], however concluded that the multiple exotherm observed during heating of a semicrystalline polymer (such as PET) sample corresponded to melting-reorganization-remelting of polymer crystals. They observed a gradual merging of the melting endotherms in PET samples as the heating rate increased from 2 K/min to 162,000 K/min. The authors argued that at commonly used heating rates, the PET chains undergo melting, and recrystallize very fast to form structures that are stable at higher temperatures. The recrystallized chains melt at higher temperatures leading to a second endotherm. However, very high heating rates prevent recrystallization process and result in only one endotherm corresponding to the melting of PET crystals.

Processing conditions such as annealing also induce significant changes in the morphology of segmented block copolymers. In combination with other techniques such as small-angle X-ray scattering, the molecular origins of thermal transitions can be accurately assigned, as will be discussed next.

1.2.2. Small Angle X-ray Scattering (SAXS)

In X-ray scattering analysis of a polymer, a collimated X-ray beam passes through the sample, usually a thin film. A characteristic scattering and/or diffraction pattern is generated, in which one or several peaks may appear that correspond to the periodicity of the morphological features in the polymer system under consideration.[21] Wide angle X-ray diffraction (WAXD) analysis of MDI-BD based polyurethanes has led to the determination of crystallinity and paracrystalline order within the crystalline domains.[22-25]

Small angle X-ray scattering analysis gives information about morphological features in the size range of approximately 2-100 nm. In a two phase system, a scattering maximum gives information about the periodicity of electron density distribution (Figure 1.3). Scattering intensity at higher angles gives information about diffuse phase boundary thickness.[5,15,26-29]

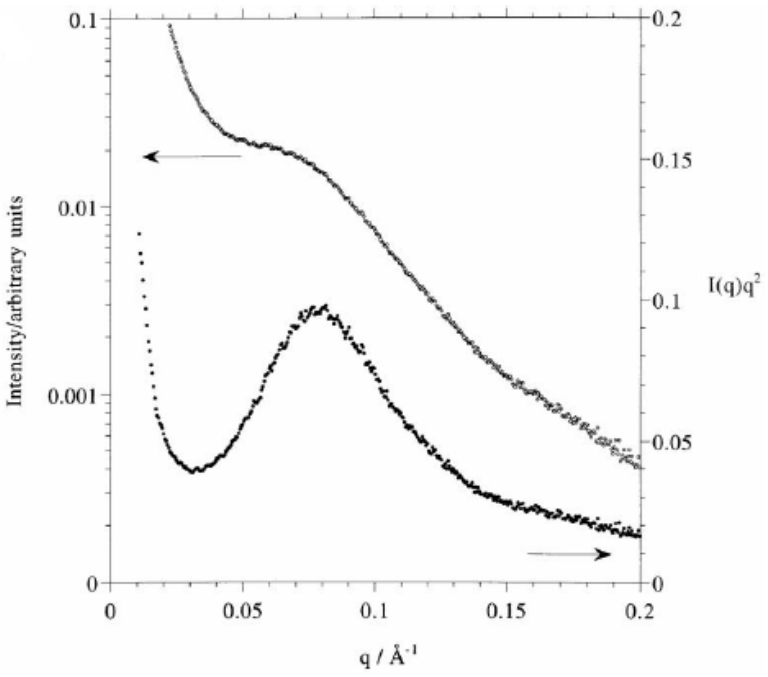

Figure 1.3: SAXS profile of poly(ether-urea) foam.[30] Reprinted from *Polymer* **2000,** *41* (7), Hamley, I. W.; Stanford, J. L.; Wilkinson, A. N.; Elwell, M. J.; Ryan, A. J., Structure development in multi-block copolymerisation: comparison of experiments with cell dynamics simulations. 2569-2576. Copyright 2000. With permission from Elsevier.

Porod[31-33] first reported and formulated scattering behavior of an ideal two-phase system with sharp phase boundaries. At large scattering vector (q) values, Porod's law states that the scattering intensity decreases proportional to the inverse of the scattering vector to the fourth power.

$$\lim_{q\to\infty} I(q) = \frac{K_P}{q^4} \tag{2}$$

Porod's constant, K_P, is an important structural parameter related to the interfacial area of phase separated domains by the following equation:

$$K_P = \left(\frac{S}{V}\right)\left(\frac{Q}{8\pi^3}\right)\varphi_1\varphi_2 \tag{3}$$

(S/V) is the surface area per unit volume of phase separated domains. The volume fractions of each phase are represented by φ_1 and φ_2, ρ_1 and ρ_2 are electron densities of each phase and Q is called scattering invariant and is calculated as follows:

$$Q = \int_0^\infty q^2 . I(q) . dq = V \emptyset_1 \emptyset_2 (\rho_{1-} \rho_2)^2 \quad (4)$$

Multiphase polymers generally do not strictly follow the Porod's law. Scattering from the randomly mixed segments (background scattering) and gradual change in the electron density across the interface (instead of a sharp phase boundary) cause deviation from Porod behavior. Ruland[34] proposed a constant value for the background scattering intensity while Vonk[35] presented a power series of q to account for the same. A number of corrections have been proposed to take into account change in electron density across the interface. Ruland[34] proposed a Gaussian smoothing function and modified Porod's law as follows:

$$I(q) = \left(\frac{K_P}{q^4}\right) \exp\left(-\sigma^2 q^2\right) \quad (5)$$

Where, σ is the interfacial thickness.

Electron microscopy was used to study the structure of microphase separated domains,[36,37,38] but imaging of individual domains of the size of few nanometers was found to be difficult. Most of the domain structure studies have employed X-ray scattering method and have resulted in the development of several morphological models of microphase separated domains (rich in hard segments). These domains will be referred to as hard domains for convenience. Bonart et al.[5] first proposed a model for polyurethane hard segments in which the hard segments were packed in a lamellar domain with chain-extended configuration. Blackwell et al.[22] reported that hard segment crystal thickness was close to the average molecular weight of the hard

segments for polyurethanes. However, Bogart et al.[39] and Koberstein and Stein[40] reported that the thickness of hard domains was close to 2 to 4 isocyanate repeat unit lengths. These results led to the development of a new morphological model, in which the hard domain thickness was proposed to be dependent on the contour length of the shortest hard segment sequence that is insoluble in soft microphase. Leung and Koberstein[41] studied a range of polyurethane compositions and reported that the hard domains were discreet when the hard segment content was approximately below 50 %. Above 50 % content, the polyurethanes showed continuous hard domain morphology. They also verified that a critical hard segment length of 3-4 isocyanate units was required to form a microphase separated hard domain. They proposed that sequences shorter than the critical segment length dissolved in the soft microphase whereas longer sequences adopted a coiled morphology allowing reentry of polymer chains into the hard domains.

1.2.3. Dynamic Mechanical Analysis (DMA)

In DMA, the polymer under study is subjected to a sinusoidal force (stress) and its response (strain) is observed as a function of time and / or temperature. The phase lag between the applied force and material strain leads to the determination of the viscosity and the amplitude of the strain leads to determination of the polymer modulus. The modulus obtained from DMA is represented by a complex equation, in which the real term is referred to as the "storage modulus" and the imaginary term is called the "loss modulus". The ratio of storage and loss modulus is called damping (tan δ), and is an important parameter to characterize various relaxation processes that occur in polymers.[42]

One of the earliest dynamic mechanical studies was reported by Pigott et al.[43] They analyzed a series of polyurethanes prepared using a variety of aromatic isocyanates, glycol chain extenders, and polyester soft segments. They concluded that the isocyanates with higher rigidity and symmetry increased the modulus of the polyurethanes. However, the glass transition temperature of the soft segments was only moderately affected. The chain extenders did not affect the mechanical properties to the same extent as that of the isocyanates, but the glycols with longer aliphatic chains yielded polyurethanes with lower modulus. They also observed that polyesters with shorter spacing between ester groups yielded polyurethanes with higher modulus at room temperature.

Several papers from Cooper and co-workers[17,19,38,39,44,45] concluded that the hard segments act as physical crosslinks and hence are responsible for unusual dynamic mechanical behavior of segmented block copolymers. In another detailed study, dynamic mechanical analysis was correlated with thermal and X-ray scattering analysis, allowing Huh et al.[46] to identify various morphological transitions in polyurethane and polyester/polyether based segmented block copolymers. Figure 1.4 shows dynamic mechanical spectra of polyester-polyurethane copolymers with increasing molecular weight of polyester segments.

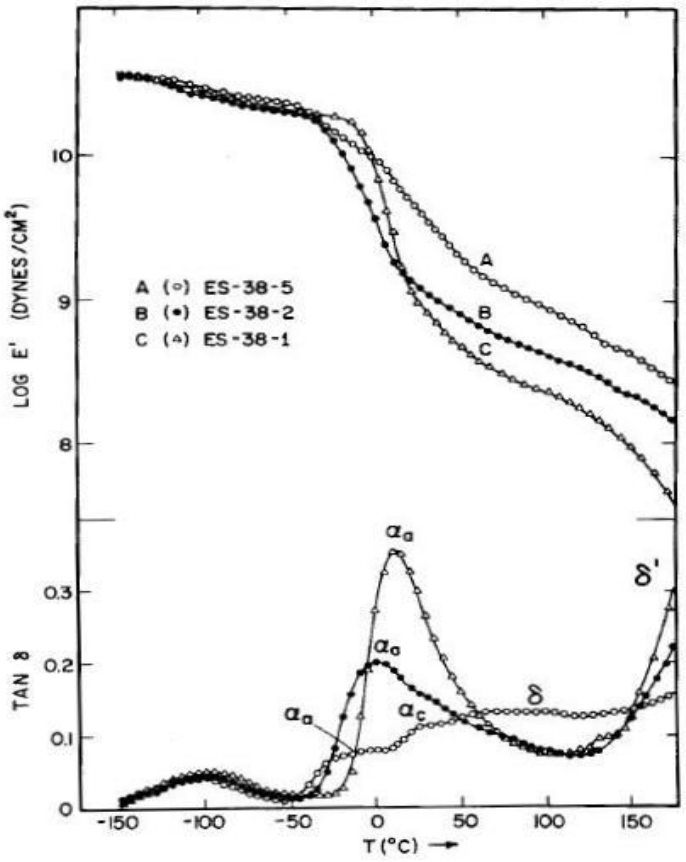

Figure 1.4: Storage modulus and tan δ spectra of various polyurethanes based on MDI-butanediol and polytetramethylene adipate.[46] Reprinted with permission from Huh, D. S.; Cooper, S. L., Dynamic mechanical properties of polyurethane block polymers. *Polymer Engineering & Science* **1971,** *11* (5), 369-376. Copyright 1971. John Wiley and Sons, Inc.

The γ relaxation centered around -100 ^{0}C was assigned to the short-range motions of methylene units. The β relaxation was assigned to the motion of amino and carboxyl groups associated with water molecules by hydrogen bonding. Relaxations α_a and α_c were attributed to glass transitions of polyester segments and melting of imperfect crystallites of either polyester or polyurethane segments. The δ and δ' relaxations were attributed to the motion of amorphous hard segments and the melting of hard segment crystals respectively.

It is evident from the literature discussed in this chapter that a segmented block copolymer is likely to exhibit better higher mechanical modulus when the number of crosslinks

i.e. the extent of microphase separation is higher at service temperatures. It is also important that the hard domains retain their structure at service temperatures. The two common approaches to affect the aggregation and stability of hard segments are annealing and introduction of ionic groups on polymer backbone, which are discussed in the next section.

1.3 Chemical and physical methods to modify morphology of segmented multiblock copolymers

1.3.1. Effect of ionic groups on the morphology and mechanical properties of segmented multiblock copolymers

The use of ion containing segmented multiblock copolymers is a field of special interest due to their applicability in biomaterials.[47,48] Dieterich et al.[49] first reviewed the syntheses of polyurethane ionomers that were obtained by reacting isocyanates with small quantities of amino-functional diols, followed by the quaternization of amines using a suitable agent (such as dimethyl sulfate). The authors also reported the synthesis of polyurethane containing negatively charged groups, such as sulfonate. Polyurethane ionomers can be water dispersible, which makes them an attractive choice for environmentally friendly polymer systems. Excellent mechanical properties of polyurethanes coupled with practically no requirements for volatile organic solvents in their processing provides a great potential for foams and coatings.[50,51]

Hwang et al.[52] studied polyurethane zwitterionomers and concluded that the polyurethanes with higher hard segment content led to greater microphase mixing. However, increasing ion content resulted in improved microphase mixing as seen by a sharper and relatively low temperature glass transition of soft segments (Figure 1.5). Higher ion content also led to a higher rubbery modulus obtained from dynamic mechanical analysis. Ionic interactions

resulted in improved cohesion in the hard segments and consequently higher softening temperatures. Improved tensile modulus was also observed for samples with higher ion content.

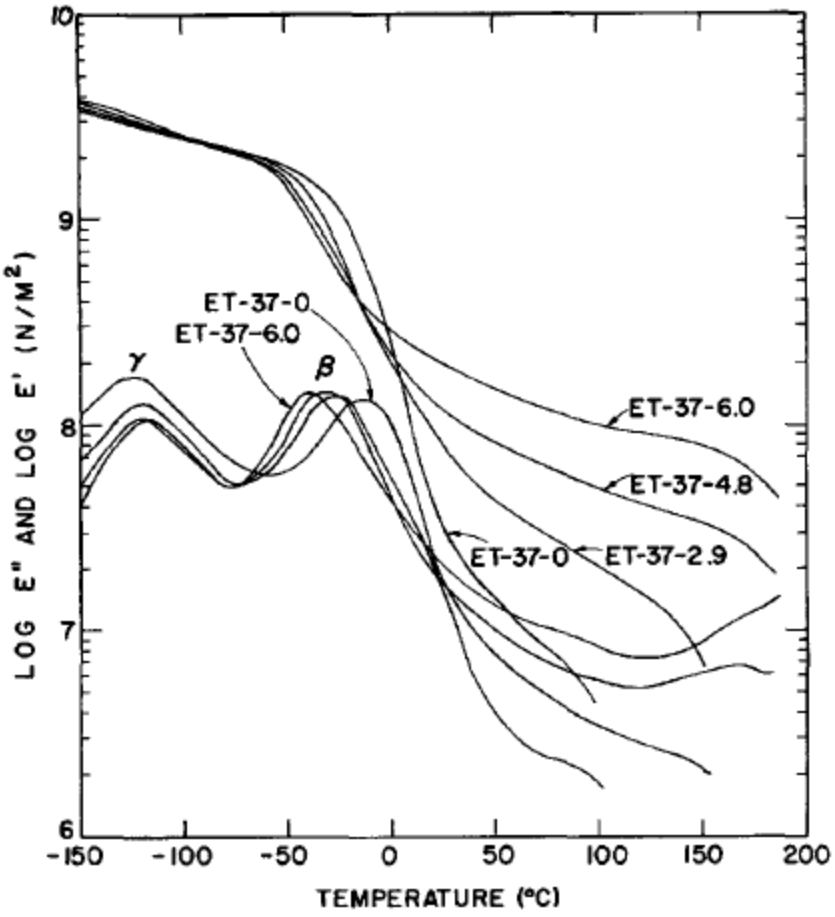

Figure 1.5: Storage and loss modulus spectra of a series of polyurethanes. ET-37-6.0 represents polyether segments, 37 % polyurethane hard segment content and 6.0 wt% sulfonate content respectively.[52] Reprinted with permission from Hwang, K. K. S.; Yang, C.-Z.; Cooper, S. L., Properties of polyether-polyurethane zwitterionomers. *Polymer Engineering & Science* **1981,** *21* (15), 1027-1036.) Copyright 1981. John Wiley and Sons, Inc.

Similar studies were carried out on sulfonate containing polyurethanes,[53,54] polyurethanes with various types and contents of soft segments,[55] polyurethanes with hard segments containing carboxyl groups,[56] cation containing polyurethanes,[57] and polyurethane-urea with soft segments containing urethane units.[58] All of these studies arrived at the same conclusion of electrostatic interaction playing a major role in development of the copolymer morphology.

Chen and Hsu[59] studied polyurethane anionomers with quaternary ammonium counterions and concluded that the size of counterions has a significant effect on morphology. The smaller counterion (tetraethylammonium) showed a greater extent of microphase separation, larger hard domain size, and higher mechanical modulus. Santerre and Brash[60] observed that polyurethanes with low ion content had an increased modulus, possibly due to better interaction between polymer chains in hard segments. However, at higher ion contents these interactions led to increased microphase mixing and subsequent loss of mechanical properties. Wei and Yu[61] reported the synthesis of polyurethane ionomers in which the ionic groups were incorporated into the soft segment. The ionomers exhibited properties similar to those which contain ionic groups in hard segments. However, increasing ion content in soft segments led to an increased microphase mixing as evidenced by broader glass transitions and increased glass transition temperature of soft segment.

Since the current research is based on segmented multiblock copolymers containing polyester hard segments, it is important to look at the effect of ionic groups present in polyester segments as well. Szymczyk and Roslaniec[62] synthesized polyester-ether ionomers in which the polyester hard segments contained dimethyl 5-sulfoisophthalate units. These ionomers did not show a significant change in the soft segment glass transition temperature, regardless of increasing ion content. This behavior was attributed to ionic interactions that restricted polyester chain mobility and prevented significant microphase mixing. Thermal analysis of these ionomers[63] showed a decrease in the polyester crystallinity with increasing ion content. Copolymers with higher ion content also showed slightly inferior mechanical properties as observed during tensile testing. It was proposed that the ion containing isophthalate units acted as defects in the regular arrangement of polyester crystals and thus caused inferior mechanical

properties. SAXS and WAXD analysis of the copolymers[64] with hard segments containing sulfonated poly (butylene terephthalate) showed decreasing crystallinity of hard segments with increasing ion content. The morphology of ion containing copolymers was very similar to the non-ionic copolymers. Based on these results it was proposed that ionic aggregates are formed inside the lamellar domains of polyester chains. However, ionic interactions were still considered to be the driving force for microphase separation.

1.3.2. Effect of annealing on the morphology and mechanical properties of segmented multiblock copolymers

Differential scanning calorimetry has been the most widely used technique for studying the effects of annealing. A number of publications by Cooper et al.[17-19,38,39,45,52,55,65-69] and Wilkes et al.[24,28] involve an extensive DSC analysis of polyurethanes with varying chemical structures and compositions. The influence of several factors, including presence or absence of hydrogen bonding, molecular weight, and the crystallinity or amorphous nature of hard and soft segments on the development of polymer morphology after thermal treatment, have been reported in the literature. DSC thermograms of polyurethanes showed multiple thermal transitions, which were manipulated by varying the annealing temperature to determine their morphological origins. In general, the peak appearing 20-50 ^{0}C above the annealing temperature was assigned to the disruption of local ordering in hard segments (Figure 1.2). The peak moved to higher temperatures with increasing annealing temperatures and eventually merged with the peak that was assigned to the disruption of long-range ordering in hard segments.[17]

Based on DSC and SAXS analysis, Leung and Koberstein[70] proposed that the high temperature transition corresponded to mixing of the two microphases. In the case of crystalline

hard segments, another peak appeared at even higher temperatures (generally above 200 ^{0}C for polyurethanes), which was assigned to the melting of hard segment crystals.

Etienne et al.[71] studied the annealing effects of amorphous polyurethanes on their dynamic mechanical properties. They observed that when the polymers were annealed above the T_g for the hard segments, the rubbery region showed a significant temperature dependence during dynamic mechanical analysis (Figure 1.6). Scattering analysis showed that annealing at higher temperatures resulted in a shift of the scattering maximum to lower angles but the scattering invariant remained relatively constant. This morphological change was attributed to coarsening of the hard segment domains.

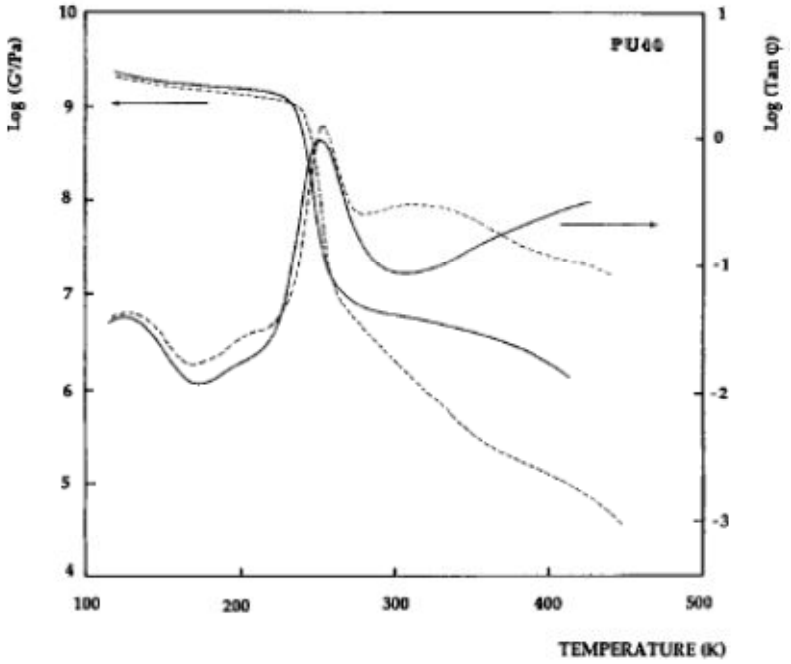

Figure 1.6: Dynamic shear modulus and tan delta spectra of a polyurethane sample. (—) as prepared sample; (···) after annealing.[71] Reprinted with permission from Etienne, S.; Vigier, G.; Cuvé, L.; Pascault, J. P., Microstructure of segmented amorphous polyurethanes: small-angle X-ray scattering and mechanical spectroscopy studies. *Polymer* **1994,** *35* (13), 2737-2743. Copyright 1994. John Wiley and Sons, Inc.

Li et al.[72] observed an increased intensity of the scattering maximum in polyurethanes with increasing annealing temperatures, suggesting a greater extent of hard segment organization and microphase separation. The scattering maximum also shifted to lower angles, which is indicative of increasing separation between microphase separated domains (Figure 1.7). The authors proposed that hard segment coils expand during the annealing process and extend, thereby increasing interdomain spacing.

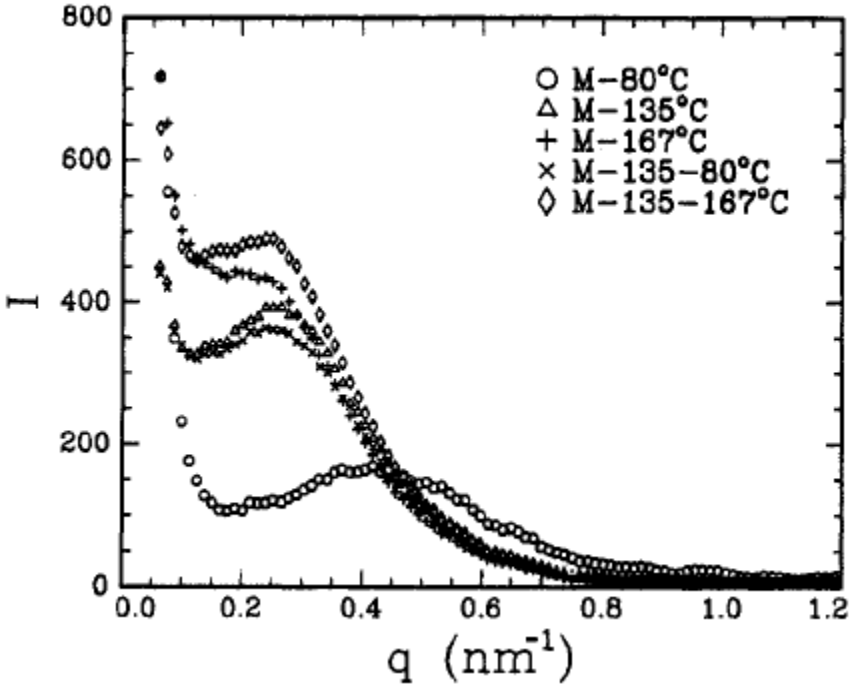

Figure 1.7: Effect of annealing on the morphology of MDI-butanediol based polyurethane with PPO-PTMO soft segments. All samples were quenched from melt and annealed at temperature/s written in the order.[72] Reprinted with permission from Li, Y.; Gao, T.; Liu, J.; Linliu, K.; Desper, C. R.; Chu, B., Multiphase structure of a segmented polyurethane: effects of temperature and annealing. *Macromolecules* **1992,** *25* (26), 7365-7372. Copyright 1992. American Chemical Society.

In conclusion, significant information about the morphology of a segmented multiblock copolymer can be obtained by thermal, scattering, and dynamic mechanical analysis. Analytical techniques – DSC, X-ray scattering and DMA can explore various morphological transitions occurring in the copolymer and by varying the processing conditions, the influence of several

characteristics of the copolymer system, such as crystallinity and ionic interactions, can be evaluated. A thorough knowledge of the relationship between block copolymer morphology and corresponding mechanical and other performance properties will enable one to tune the copolymer performance as per the application requirements.

Although a large quantity of literature is available on the kinetics of microphase separation in segmented block copolymers,[24,27,28,73-79] it is out of the scope of this study and thus not discussed in this review. Techniques such as transmission electron microscopy[36-38] and rheometry[80-83] have been used extensively to study the morphology of segmented multiblock copolymers. These techniques are out of the scope of this study and hence not discussed in the review.

Chapter 2: Materials and Analytical Techniques

The polyester polyols and copolyesters were synthesized by Zhang and Long.[84] Details about the raw materials and synthetic methods have been reported elsewhere. Only a brief description of these materials is included in this section.

2.1 Materials

2.1.1 Poly(CBDO-DMCD) Polyester Polyol

Poly(CBDO-DMCD) polyester polyol, which is the hard segment in the segmented copolyesters, was synthesized by reacting dimethyl-1,4-cyclohexane dicarboxylate (DMCD) (99% trans) with excess 2,2,4,4-tetramethyl-1,3-cyclobutanediol (CBDO)(45:55 cis:trans) in the presence of a dibutyltin oxide catalyst. The reaction scheme is given below.

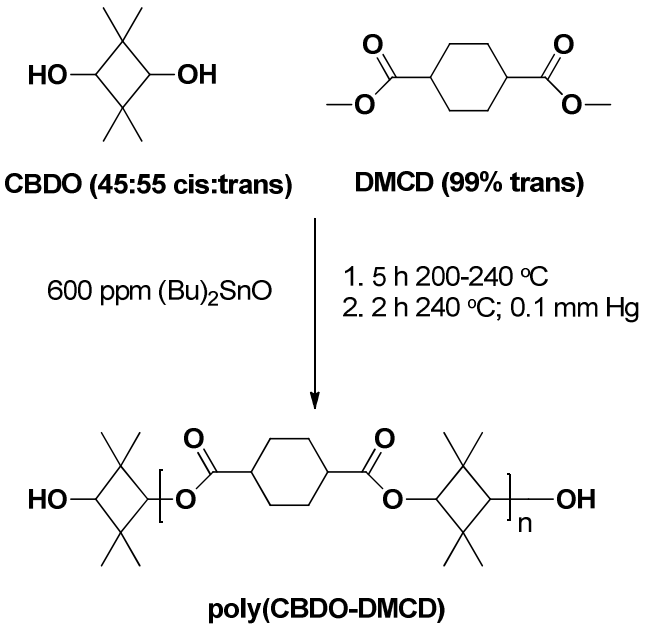

Scheme 2.1: Synthesis of poly(CBDO-DMCD) polyol.[84]

2.1.2 Poly[(CBDO-DMCD)-*co*-(DEG-DMAp)] Segmented Copolyesters

Poly[(CBDO-DMCD)-*co*-(DEG-DMAp)] segmented copolyesters were synthesized by reacting appropriate quantities of poly(CBDO-DMCD), diethylene glycol (DEG), and dimethyl adipate (DMAp) at 180 °C for 5 hours in the presence of catalysts dibutyltin oxide and titanium tetra(isopropoxide) in an inert environment. The chemical structure of the resulting polyester is shown below.

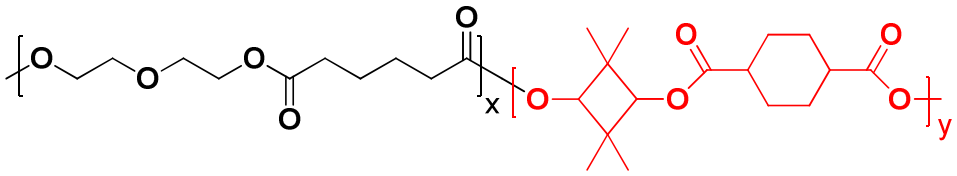

Figure 2.1: Poly[(CBDO-DMCD)-*co*-(DEG-DMAp) segmented copolyesters.[84]

2.1.3 Poly(sCBDO-DMCD) - sulfonated polyester polyol

Sulfonate groups were incorporated into the hard and soft segments by adding sodium sulfoisophthalate (Na-SIP) as a co-monomer during the polyester synthesis.

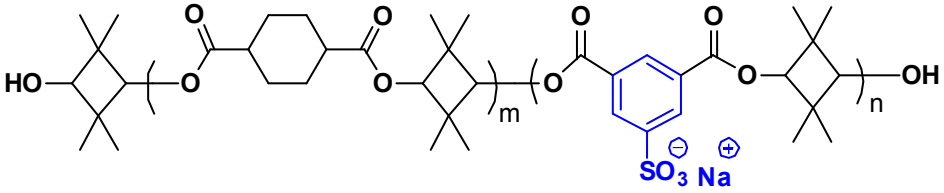

Figure 2.2: Sulfonate containing poly(sCBDO-DMCD) polyester polyols.[84]

2.1.4 Sulfonated Segmented Copolyesters

Polyols containing 1, 3, and 5 mol% Na-SIP were synthesized and further reacted with dimethyl adipate and diethylene glycol to generate a series of copolyesters containing varying sulfonate content. The chemical structure of the copolyester is shown in Figure 2.3.

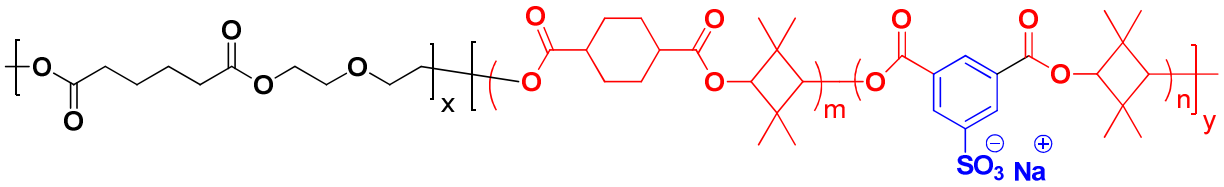

Figure 2.3: Sulfonated hard segment containing segmented copolyesters.[84]

Another series of sulfonated copolyesters was synthesized that contained Na-SIP in the soft segments. The chemical structure of this type of copolyesters is shown in Figure 2.4. This series contained soft segments with 1, 3 and 5 mol% Na-SIP and the hard segment content was maintained at 30 wt. %

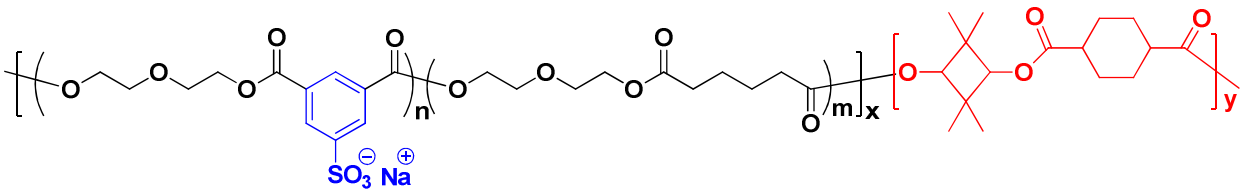

Figure 2.4: Sulfonated soft segment containing copolyesters.[84]

2.2. Nomenclature

Since several copolyesters (non-sulfonated and sulfonated) are mentioned frequently in the following chapters, the following nomenclature has been used to address each of the copolyesters.

Table 2.1: List of non-sulfonated and sulfonated segmented copolyesters and their composition

Copolyester	Hard Segment (wt. %)	Sulfonation in Hard Segment (mol %)	Sulfonation in Soft Segment (mol %)
0s-30	30	0	0
1s-30	30	1	0
3s-30	30	3	0
5s-30	30	5	0
0s-40	40	0	0
1s-40	40	1	0
3s-40	40	3	0
1s-30_ss	30	0	1
3s-30_ss	30	0	3
5s-30_ss	30	0	5

For example, **3s-30** means that the copolyester contains 30 wt. % hard segments and hard segments contain 3 mol % of Na-SIP. In case of **3s-30_ss**, the copolyester contains 30 wt. % hard segments, and the term "ss" means that the soft segments contain 3 mol % of Na-SIP. In all copolyesters containing sulfonated soft segments, the hard segments do not contain any Na-SIP.

2.3. Molecular weight determination

Molecular weights of the polyols and copolyesters were determined from ^{1}H NMR and SEC (polystyrene standard) analysis. The following table shows M_n and M_w values of non-sulfonated polyol and copolyesters determined by different methods.

Table 2.2: Molecular weights of non-sulfonated polyol and copolyesters.[84]

Polymer Sample	M_n[a] (g/mol)	M_n[b] (g/mol)	M_w[b] (g/mol)	M_w/M_n[b]
Poly(CBDO-DMCD)	4020	3449	4896	1.22
0s-30	-	29,300	41,300	1.41
0s-40	-	31,500	50,000	1.59

[a]Calculated from ^{1}H NMR spectroscopy

[b]Chloroform SEC: Refractive index detector (30 °C) with polystyrene standard.

The ion containing polyols and copolyesters formed aggregates in SEC solvents. ^{1}H NMR spectroscopy was used to characterize low molecular weight polyols. The following table shows the molecular weights of sulfonated polyols poly(sCBDO-DMCD) determined using ^{1}H NMR spectroscopy.

Table 2.3: Molecular weight of sulfonated polyester polyols (hard segments).[84]

Mol % Na-SIP in Hard Segment	M_n (g/mol)
1	3,500
3	3,410
5	3,330

2.4. Copolyester Film casting

The non-sulfonated copolyesters were dissolved in chloroform and films were cast at room temperature, on a silicon coated substrate using a film applicator. The sulfonated copolyesters were dissolved in a 90:10 (v/v) mixture of chloroform and methanol and films were cast at room temperature. The films were then annealed under reduced pressure for 1 day before subjecting them to thermal and morphological analysis. A range of temperatures (25-160 °C) was used for the annealing of copolyesters. The particular temperatures were chosen due to appearance of a thermal transition near that temperature. E.g. in the case of samples annealed at 80 °C, a broad endotherm was observed around 135 °C. Consequently, the samples were annealed at 135 °C.

2.5. Characterization Techniques

2.5.1 Differential Scanning Calorimetry (DSC)

A TA instruments DSC Q-2000 model was used for the DSC measurements. The instrument was calibrated using indium and sapphire standards and is equipped with an RCS cooling system that has a lower temperature limit of -90 ^{0}C. The temperature range for all analyses was kept at -90 to 200 ^{0}C. For heat capacity determination, the samples were heated at 5° C/min rate. In all other experiments a 20 ^{0}C/min heating rate was employed.

2.5.2 Small Angle X-ray scattering (SAXS) and Wide Angle X-ray Diffraction (WAXD)

The SAXS measurements were carried out using a Rigaku S-Max 3000 3 pinhole system. X-rays of wavelength 0.154 nm were generated by a rotating copper anode. The scattering data was obtained for each sample over a period of 1 hour and a 2-dimensional scattering pattern was generated using SAXSGUI software. The WAXD data were obtained using an image plate and an exposure time of 30 minutes. The two-dimensional SAXS/WAXD data were radially integrated using SAXSGUI software.

The WAXD patterns of the hard segment powders were obtained using a Rigaku Miniflex II Desktop X-ray Diffractometer with Cu Kα radiation (λ = 0.154 nm). The samples were scanned at the rate of 0.5 °/min and at a step size of 0.05 °.

The real-time variable temperature SAXS measurements were carried out at Advanced Photon Source (APS), Argonne National Laboratory (Beamline 5-ID DND-CAT). The X-ray wavelength was 0.07293 nm. Scattering from a silver behenate standard was used to calibrate the sample-to-detector distance. SAXS images were obtained using a low-noise, Mar USA Inc,

162 mm, marCCD camera, with a 4 second exposure time. All SAXS data were corrected for sample thickness, sample transmission and background scattering.

2.5.3 Dynamic Mechanical Analysis (DMA)

DMA measurements of copolyesters were carried out on TA instruments DMA Q 800 using a film tension clamp. The samples were scanned at 1Hz frequency, and from -120 ^{0}C up to the yield temperature.

Chapter 3: Thermal and Morphological Analysis of Poly[(CBDO-DMCD)-*co*-(DEG-DMAp)] Copolyesters

3.1. Introduction

Segmented multiblock copolyesters can undergo hydrolytic degradation and hence can be utilized in biomedical applications and recyclable products.[85-87] However, in the case of polyester-polyester copolymers, both segments may undergo transesterification.[12,88] The copolymers under consideration consist of a polyester segment poly(CBDO-DMCD) that contains sterically hindered hydroxyl groups, and are chain-extended by monomers that form the low-T_g polyester segments (soft segments). The transesterification resistance of poly(CBDO-DMCD) segments was to 1-dodecanol and 2-dodecanol was observed in the temperature range 160-220 °C.[84] ^{1}H NMR analysis of poly(CBDO-DMCD) segments showed a decrease in the number average molecular weight (M_n) when the segments were reacted with 1-dodecanol (less sterically hindered) and practically no change in M_n when the segments were reacted with 2-dodecanol (more sterically hindered).

Segmented block copolymers exhibit a microphase separated morphology, which results in their unique mechanical properties.[5] Hence, to predict the mechanical properties, it is essential to understand the morphology of the poly[(CBDO-DMCD)-co-(DEG-DMAp)] copolyesters. The current chapter addresses fundamental questions such as whether these copolyesters exhibit a microphase separated morphology, how do the different polyester segments aggregate, and how stable are the microphase separated domains. The reported data obtained from thermal and scattering analysis will lead to significant understanding of the copolyester morphology.

3.2. Differential Scanning Calorimetry (DSC) Analysis

3.2.1 Thermal Transitions in Copolyesters and Pure Hard and Soft Segments

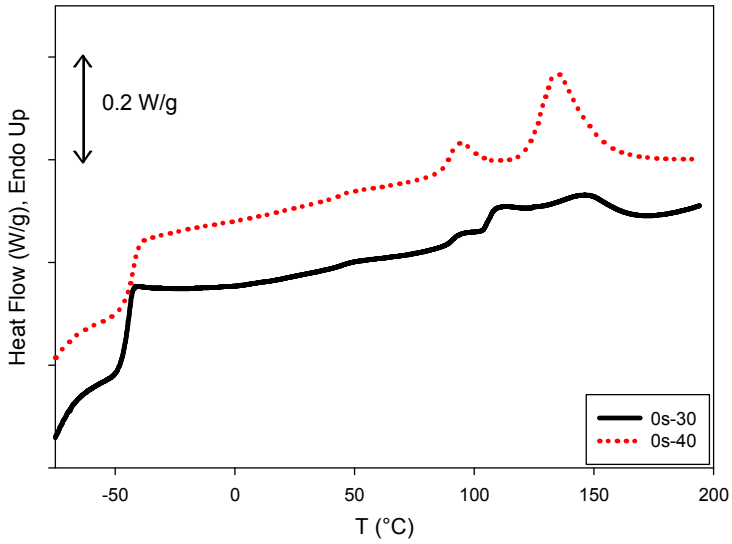

Figure 3.1: DSC thermograms of **0s-30** and **0s-40** copolyesters annealed at 80 °C for 24 hours. 1st heat scan, heating rate: 20 °C/min. Thermograms shifted along Y-axis.

DSC thermograms of solution cast copolyesters annealed at 80 °C show three prominent transitions - the low temperature glass transition and endothermic transitions (T_I and T_{II}) centered around 100 °C and 150 °C, respectively. A weak transition around 50 °C is also visible. The copolyester with higher hard segment (HS) content (40 wt. %) shows more prominent transitions. Segmented block copolymers microphase separate into hard and soft microphases; the hard domains are rich with the hard segments (high T_g segments) and act as physical crosslinks between soft segments. With increasing hard segment content, the number of these crosslinks also increases. By carrying out thermal analysis of the copolyesters and the constituent "hard" and "soft" (lower T_g) segments (SS), molecular origins of these transitions can be determined which would lead to a better understanding of the copolyester morphology.

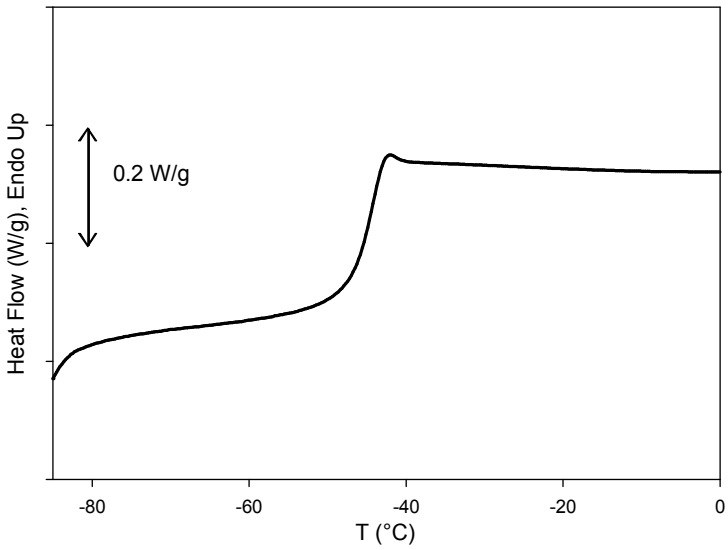

Figure 3.2: DSC thermogram of DEG-DMAp soft segments (2nd heat scan). 1st and 2nd scan heating rate: 20 °C/min. 1st scan cooling rate: 40 °C/min.

Figure 3.2 shows the T_g of the pure soft segment (DEG-DMAp) around -45 ^{0}C, which is close to the low temperature transition observed in the copolyesters (~ -43 °C), hence the low temperature transition, can be assigned to the T_g of soft segments in the soft microphase.

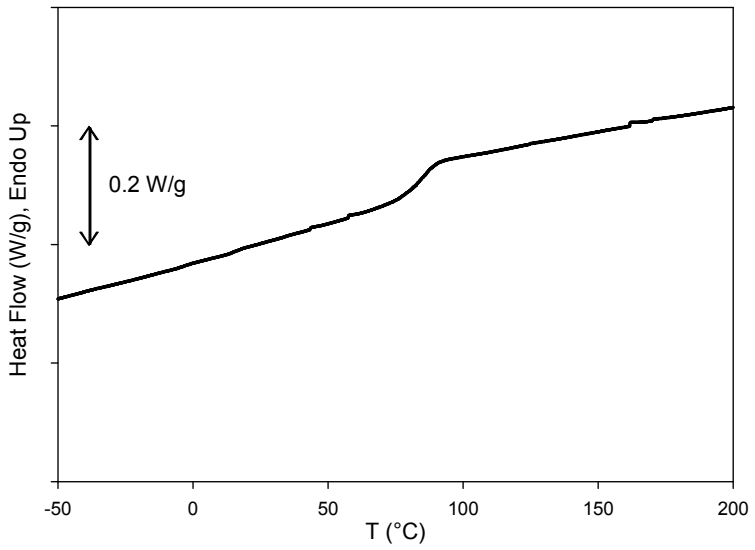

Figure 3.3: DSC thermogram of poly(CBDO-DMCD) polyol (2nd heat scan). 1st and 2nd scan heating rate: 20 °C/min. 1st scan cooling rate: 40 °C/min.

Figure 3.3 shows the T_g of the pure hard segment poly(CBDO-DMCD) around 85 ^{0}C. However, this transition is not seen clearly in the copolyester thermograms because of two factors. First, the heat capacity change associated with the glass transition of hard segments is significantly lower than that of the soft segments. Second, the hard segments contribute only 30 % of the total weight of the copolyester and hence the corresponding heat capacity change (ΔC_P) becomes even smaller. Detection of such a small heat capacity change becomes difficult with DSC.

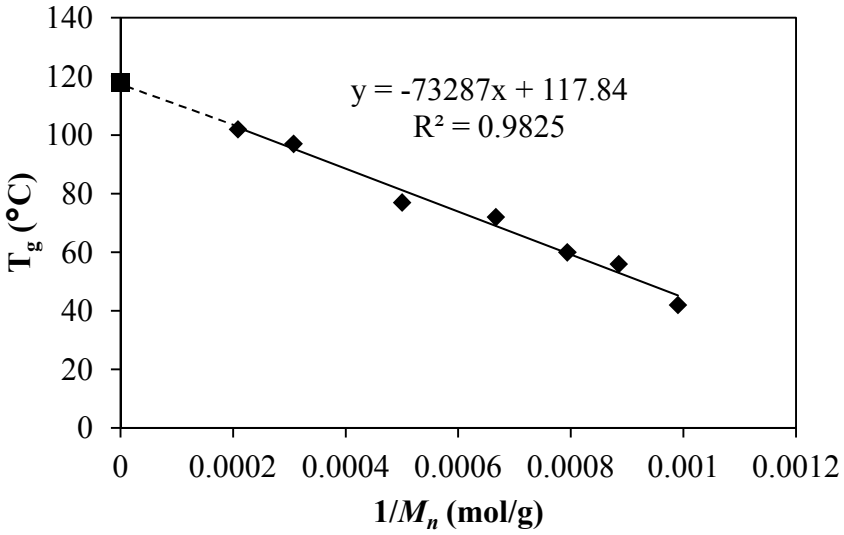

Figure 3.4: Effect of poly(CBDO-DMCD) M_n on T_g determined by DSC analysis.[84] (◆) Experimental data obtained during 2nd heat scan at 10 °C /min rate (heating and cooling). (■) Extrapolated T_g obtained using Flory-Fox equation. Reprinted with permission from Zhang M.; Moore, R. B.; Long, T. E.; *Journal of Polymer Science Part A: Polymer Chemistry*. Copyright 2012, John Wiley and Sons, Inc.

Fox and Flory[89] reported an asymptotic relationship between the molecular weight (chain length) of polystyrene and its glass transition temperature based on viscosity and specific volume measurements. The relationship is mathematically expressed as follows.

$$T_g = T_\infty - \frac{K}{M_n} \quad (1)$$

Where, K is a constant and T_∞ is the limiting value of T_g.

Figure 3.4 shows the linear plot of T_g versus inverse of the M_n of poly(CBDO-DMCD) homologues. Using the above equation, T_g of high molecular weight poly(CBDO-DMCD) was estimated to be 118 °C.[84]

3.2.2 Quench-isothermal Analysis

In quench-isothermal analysis, all samples were held at 200 °C (well above T_{II}) for 5 minutes to erase previous thermal history. Samples were then quickly cooled to the desired temperature and held isothermally for 1 hour, after which they were quickly equilibrated to -90 °C for 5 minutes. Samples were then heated up to 200 °C at 5 °C/min rate.

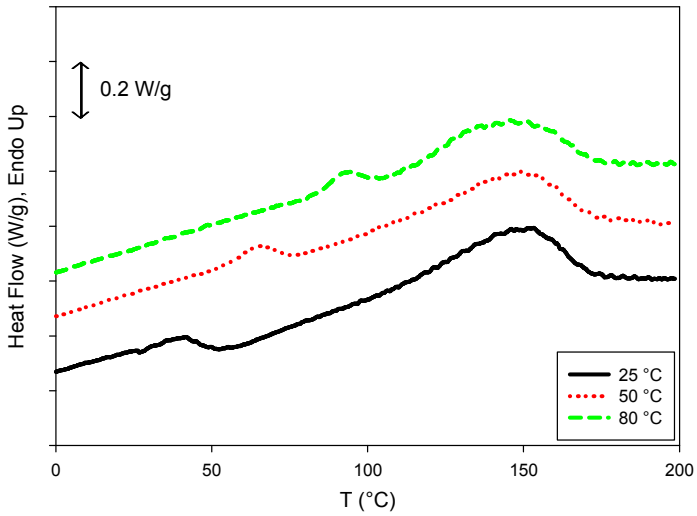

Figure 3.5: Effect of quench temperature on T_I in **0s-30**. Thermograms shifted along Y-axis.

In Figure 3.5, the endothermic transition (T_I) appears consistently 20-30 ^{0}C above the annealing temperatures of 25, 50, and 80 °C. The shift of this peak is similar to that observed in the polyurethane elastomers, in which T_I was attributed to the local ordering of hard segments as a result of annealing. Annealing treatment results in a more ordered arrangement of the hard segments, which dissociate 20 to 30 °C above the annealing temperature. The transition observed around 100 °C in Figure 3.1 is thus due to melting of the hard segment ordered structures. Also, the weak transition around 50 °C is due to room temperature annealing that occurred when samples were stored at room temperature before the DSC analysis. Figure 3.5 shows that

annealing times on the order of 1 hour are sufficient to induce morphological changes in the copolyesters.

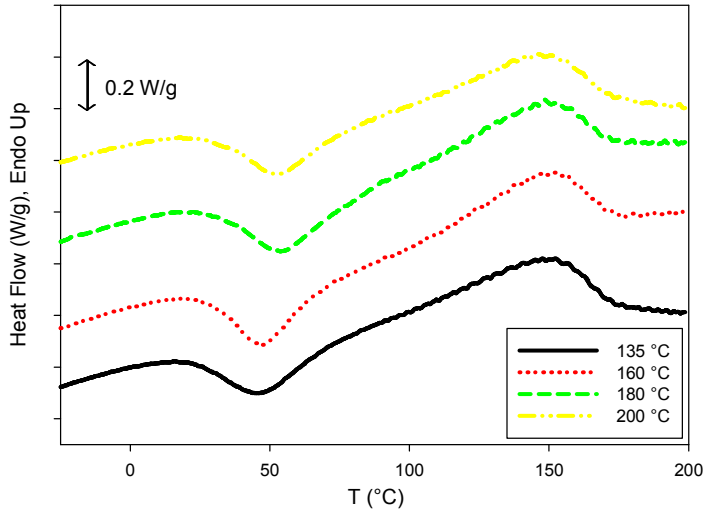

Figure 3.6: Effect of quench temperature on thermal behavior of **0s-30**. Quench temperatures are shown in the legend. Thermograms shifted along Y-axis.

When samples are quenched to 135 °C or higher temperatures from 200 °C, and subsequently quenched below soft-segment T_g, the copolyester samples show an exothermic transition during the heating scan (Figure 3.6). The onset of this transition is around 25 °C, which is approximately 60 °C above the soft segment T_g observed for each sample. Leung and Koberstein[70] observed a similar exothermic transition for melt-quenched polyurethanes and the authors attributed the exotherm to spontaneous microphase separation in a homogeneous system. Hence, the presence of exothermic transitions in copolyester samples suggests that the samples exhibit significant microphase mixing at temperatures in the range of 135 °C-200 °C. However, a similar exotherm is observed when semicrystalline polymers undergo cold crystallization.[90-92]

Table 3.1 : Enthalpy changes of exothermic and endothermic transitions in samples quenched from 200 °C to -90 °C. Samples heated at 5 °C/min rate.

Sample	ΔH_{exo} (J/g)	ΔH_{endo} (J/g)
0s-30	6.3 ± 0.8	7.7 ± 0.2
0s-40	6.0 ± 0.9	7.9 ± 0.9

Table 3.1 shows enthalpies of exothermic and endothermic transitions observed in **0s-30** and **0s-40** samples. Kusy[93] observed that isotactic PMMA samples containing small crystalline fractions (~0.05 as determined by WAXD analysis) had enthalpies of melting in the same range as those of ΔH_{endo} in **0s-30** and **0s-40**. This data suggests that the copolyesters undergo cold crystallization and hence, demixing of hard and soft segments around 50 °C. The crystalline hard segments then undergo the melting transition around 150 °C.

3.2.3 Microphase separation in Copolyesters and the Soft Segment T_g

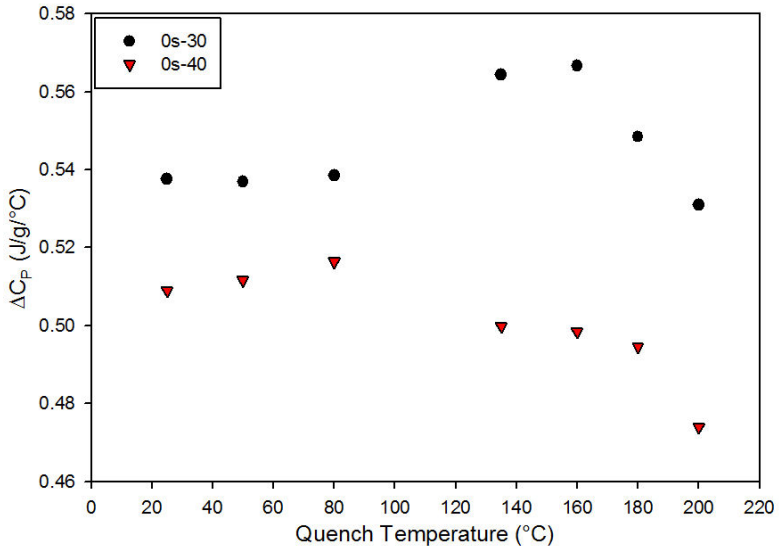

Figure 3.7: Effect of quench temperature on ΔC_P associated with soft segment glass transition in **0s-30** and **0s-40**. (Standard deviation ~ 4%)

The change in heat capacity (ΔC_P) of the copolyester sample during the soft segment glass transition is a measure of the number of soft segment chains undergoing the transition. Camberlin and Pascault[16] observed that in partially microphase separated polyurethanes, the presence of hard segments in the soft microphase did not significantly affect the soft segment ΔC_P measurements. Hence, ΔC_P could be used to represent the fraction of soft segments microphase separated from hard segments. Figure 3.7 shows the effect of the quench temperature on ΔC_P measurements. In the case of **0s-30**, the ΔC_P values gradually decrease when quench temperature increases from 160 °C to 200 °C. In the case of **0s-40**, the ΔC_P values gradually decrease with increasing quench temperature and show a significant drop in ΔC_P for samples held at 135 °C and above. The decrease in ΔC_P suggests that the fraction of soft segments in the soft microphase is decreasing.

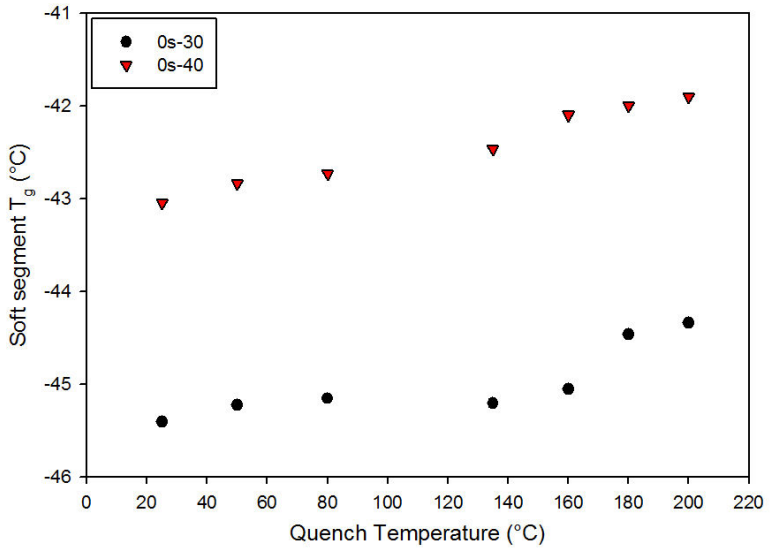

Figure 3.8: Effect of quench temperature on soft segment T_g in **0s-30** and **0s-40**. (Standard deviation ~ 4%)

Figure 3.8 shows an increase in the soft segment T_g with increasing quench temperatures above 135 °C. The onset temperature of 135 °C is close to the onset of the T_{II} transition observed in Figure 3.1. In a partially mixed soft microphase, the movement of soft segments is restricted by the hard-soft segment junctions; thus, the soft segment T_g is greater than that of the pure soft segments. As more and more hard segments mix with the soft segments, the number of these junctions increases resulting in a more restricted mobility and a higher T_g of the soft segments. However, the strength of interactions between hard and soft segments also affects the increase in T_g values. Brunette et al.[94] observed practically no effect of composition on the polyurethanes based on polybutadiene soft segments, suggesting negligible interactions between the hard and soft segments and hence a complete microphase separation. Therefore, the gradual increase in the soft segment T_g observed in Figure 3.8 indicates increasing microphase mixing in both copolyesters.

3.3. X-ray scattering and Diffraction Analysis

3.3.1 Microphase Separation in Copolyesters

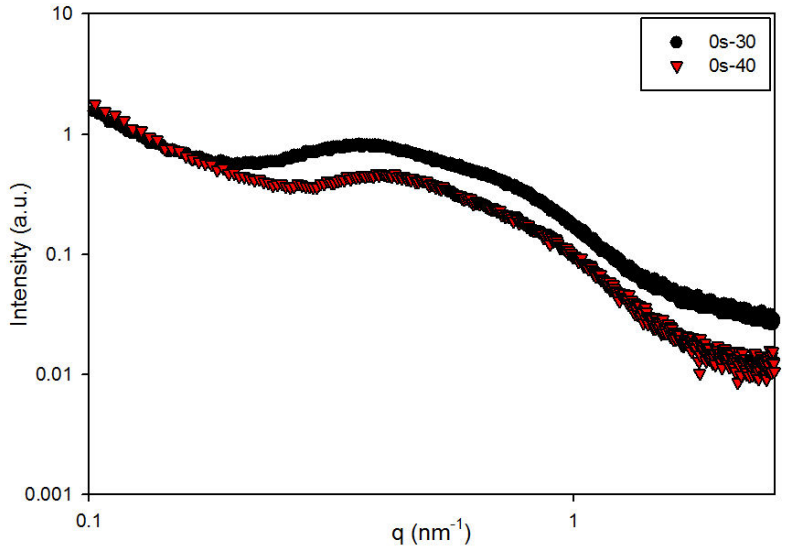

Figure 3.9: SAXS profiles of **0s-30** and **0s-40** annealed at 80 °C for 24 hours.

The SAXS profiles of copolyesters show a broad peak which is an indication of a wide distribution of distances between microphase separated domains (Figure 3.9). In the Lorentz-corrected profiles (Figure 3.10), two maxima are observed for both samples. For **0s-30** and **0s-40** samples respectively, the first maximum is observed around 0.39 nm^{-1} and 0.46 nm^{-1}, and the second maximum is observed around 0.80 nm^{-1} and 0.89 nm^{-1}. The periodicity of scattering peaks suggests lamellar morphology of the microphase separated domains; however the maxima are not very distinct due to broad scattering pattern. Hence, it can be concluded that the microphase separated domains lack a highly regular arrangement.

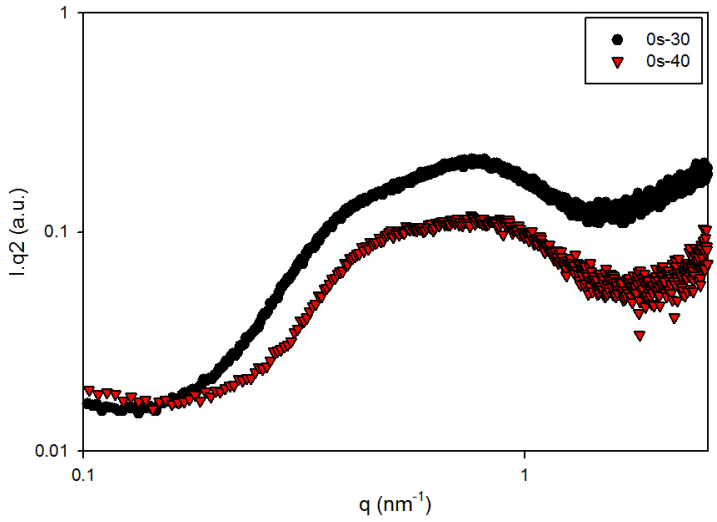

Figure 3.10: Lorentz-corrected SAXS profiles of **0s-30** and **0s-40** annealed at 80 °C (24 hours).

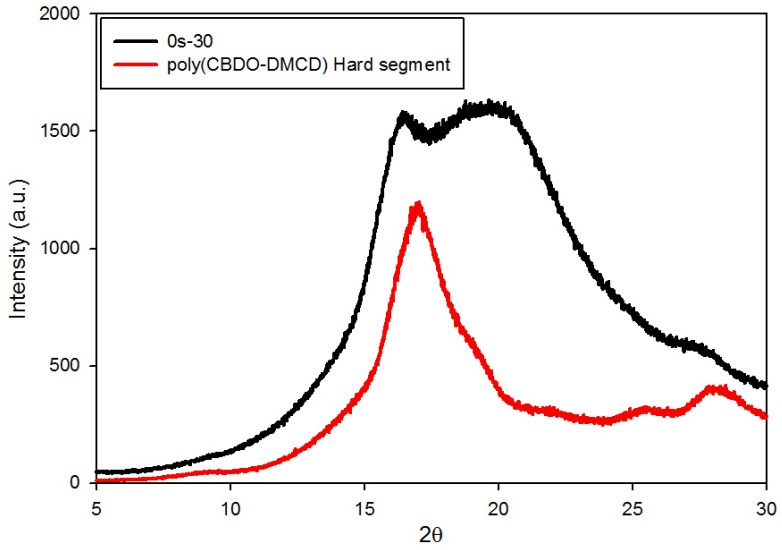

Figure 3.11: Wide angle X-ray diffraction (WAXD) profiles of solution cast **0s-30** copolyester and poly(CBDO-DMCD) hard segment.

A solution of pure hard segment in chloroform, when dried onto a substrate, yielded a brittle and opaque solid. The solid was finely ground and the powder was subjected to WAXD analysis. Figure 3.11 shows a peak near 17° 2θ in diffraction patterns of pure hard segment and solution cast copolyester. This peak suggests that hard segments are crystalline and that they

crystallize when incorporated into the copolyester as well. However, the peak is broad, which means that the crystals are disordered or small.

3.3.2 Variable-temperature X-Ray Scattering and Diffraction Analysis

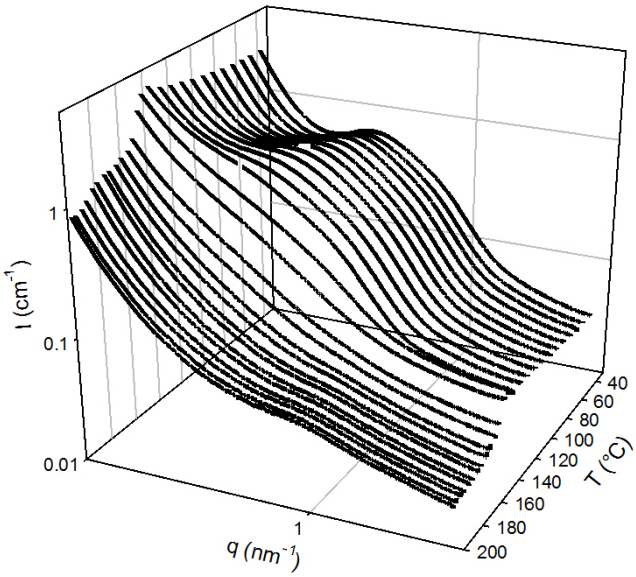

Figure 3.12: SAXS profiles of **0s-30** recorded at various temperatures during a heating ramp.

The **0s-30** sample was subjected to a variable temperature SAXS analysis. Figure 3.12 shows that the broad scattering peak disappears over the temperature range of 130-170 °C. This scattering maximum appears due to the electron density difference between hard and soft microphases and corresponds to the average distance between microphase separated hard domains. Thus, the disappearance of the scattering maximum indicates the disappearance of the microphase separated domains.

For a two-phase system with sharp phase boundaries and no fluctuations in the electron density of each phase, the scattering invariant is proportional to the volume fractions of each

phase (φ_1 and φ_2) and the square of the difference between electron densities of each phase (ρ_1 and ρ_2). Mathematically, the invariant is described as follows:

$$Q = \int_0^\infty q^2.I(q).dq = V\emptyset_1\emptyset_2(\rho_{1-}\rho_2)^2 \quad (2)$$

Hence, the experimental data was corrected for density fluctuations (i.e. background scattering intensity) and phase boundary thickness, as described by Koberstein and Stein[95] using Porod's law, which is described by the following equation:

$$\lim_{q\to\infty}[K_P - (I - I_b)q^4 \exp(\sigma^2 q^2)] = 0 \quad (3)$$

Where, K_P is Porod's constant, I is the recorded scattering intensity, I_b is the background scattering intensity, and σ is the interfacial thickness.

The Figure 3.13 shows a plot of the product of scattering intensity (I) and fourth power of scattering vector (q^4) against the fourth power of scattering vector (q^4). According to Porod's law, at high scattering vectors, the scattering intensity is proportional to the fourth power of scattering vectors and thus the $I.q^4$ vs. q^4 plot should be a straight line. In the current analysis, the background scattering (I_b) intensity was considered a constant[5] and determined as the slope of the straight line (linear fit) shown in Figure 3.13. K_P was determined as the Y-intercept of the straight line.

Figure 3.14 shows a plot of $\ln[(I-Ib).q^4]$ versus q^2. The refined Porod's constant K_P was calculated by taking exponential of the Y-intercept of the straight line (linear fit), and σ^2 was determined as the negative slope of the straight line (linear fit).

Using Porod's law, the scattering intensities at higher scattering vectors (beyond the experimental range) were estimated (down to 10^{-7} range) and used along with the corrected

experimental intensities to calculate the scattering invariant at each temperature (Figure 3.15) using equation (2).

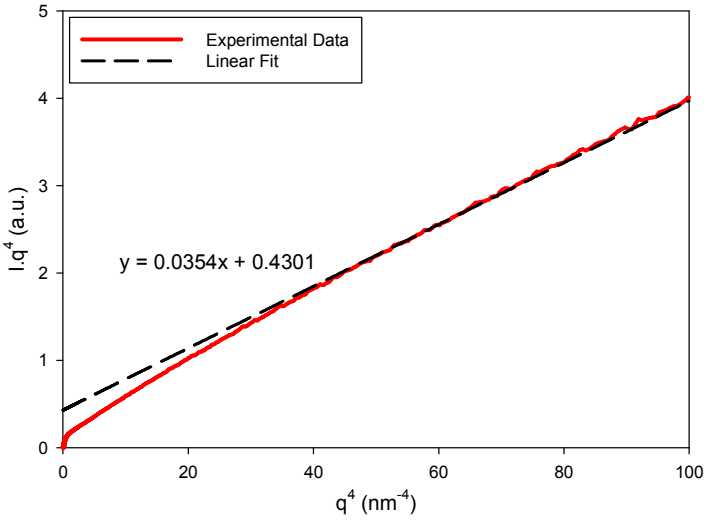

Figure 3.13: Plot of $I.q^4$ vs q^4 for the **0s-30** sample measured at 30 °C during variable temperature analysis. I_b – slope of the straight line, K_P – Y-intercept of the straight line.

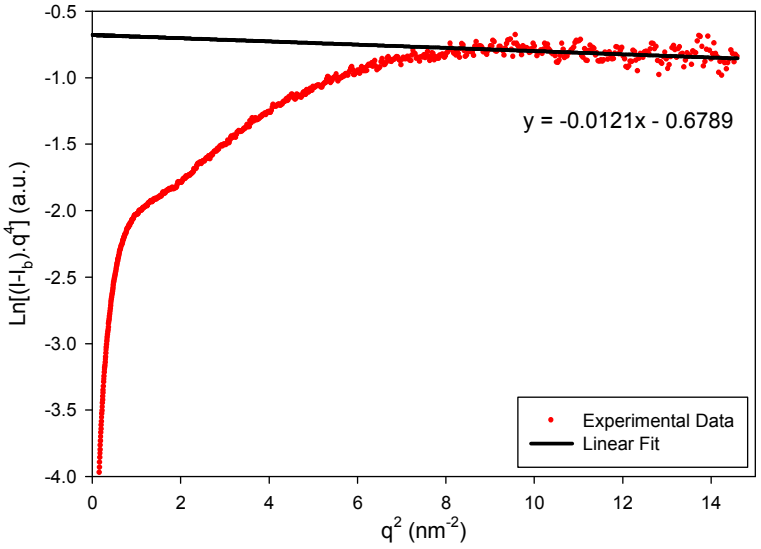

Figure 3.14: Plot of $\ln[(I-Ib).q^4]$ versus q^2 of **0s-30** sample measured at 30 °C during variable temperature analysis. σ^2 – negative slope of the straight line. Refined K_P – exponential of Y-intercept of the straight line.

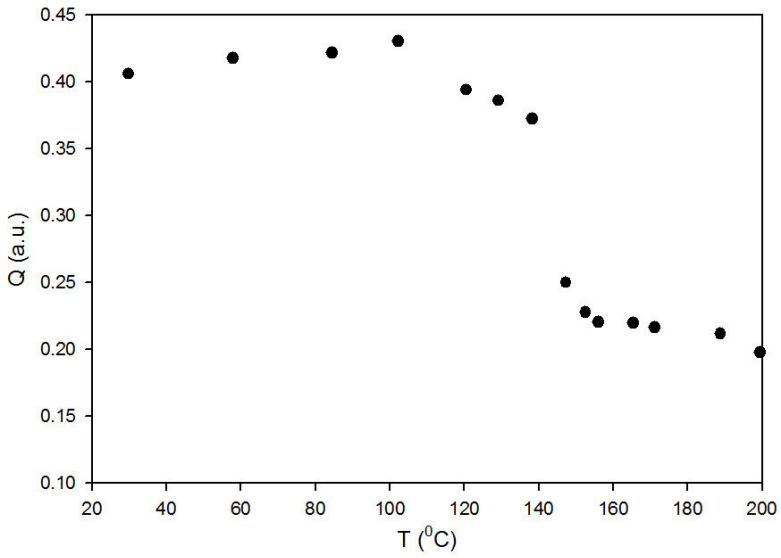

Figure 3.15: Scattering invariant (Q) of **0s-30** copolyester calculated at various temperatures. Data corrected for background scattering and interfacial thickness.

The microphase separated domains rich with the hard or soft segments exhibit a difference in electron densities due to the chemical structure of the predominant segments in each microphase. A decrease in the scattering invariant above 130 ^{0}C suggests diminishing average electron density difference between two microphases and/or change in the volume fractions of each phase i.e. microphase mixing. The decreasing difference can be accounted by two phenomena. First, as the temperature increases, the hard segment crystals melt and hence the electron density of the hard segment decreases sharply. Second, as hard segments mix with the soft microphase and vice versa, the average electron density of each microphase would change and the difference between the two microphases would reduce as they get richer with the other type of segments. Microphase mixing will also lead to change in the volume fractions of each phase which may also account for the decreasing invariant values. The scattering invariant decreases sharply over the temperature range of 130-160 ^{0}C, which overlaps with that for the T_{II} transition observed in DSC thermograms. Thus, the high temperature endothermic peak observed

in DSC thermograms may involve melting of hard segment crystals and subsequent mixing of two microphases.

The scattering invariant calculated at temperatures above T_{II} does not go to zero, thus not following equation (2) precisely. One possibility is that the copolyester is not a one-phase system at 200 °C during the heating scan ($\rho_1 \neq \rho_2$). The other possibility is that the correction applied to account for the background intensity and interfacial thickness may not be appropriate. The scattering data is collected over a limited range of scattering angles and hence the linear fits in Figures 3.13 and 3.14 are only approximations, which may also lead to deviation from the ideal behavior.

Ryan et al.[83] reported the X-ray scattering and rheological analysis of amorphous polyurethanes with 4,4'-diphenylmethane diisocyanate and 1,4-butanediol hard segments, and poly(oxyethylene-b-oxypropylene) soft segments. They observed that the scattering maximum disappeared over the same temperature range that of a large decrease in the material modulus. The authors assigned the change in the morphology to order-disorder transition (ODT).

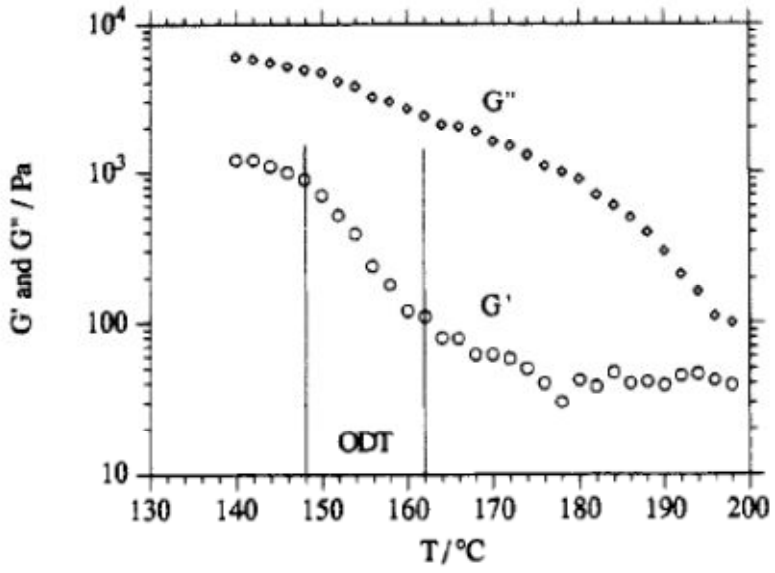

Figure 3.16: Parallel plate storage (G') and loss (G") modulus of compression molded polyurethane (50 wt. % hard segments).[83] Ryan, A. J.; Macosko, C. W.; Bras, W., Order-disorder transition in a block copolyurethane. *Macromolecules* **1992,** *25* (23), 6277-6283. Copyright 1992, with permission from Elsevier

The order-disorder transition involves destruction of the long-range order within polymer segments, but may not necessarily result in a single-phase system.[96] This argument also supports the observed scattering invariant not becoming zero above T_{II} transition (Figure 3.15), as there may not be a complete homogenization of two phases above T_{II} transition.

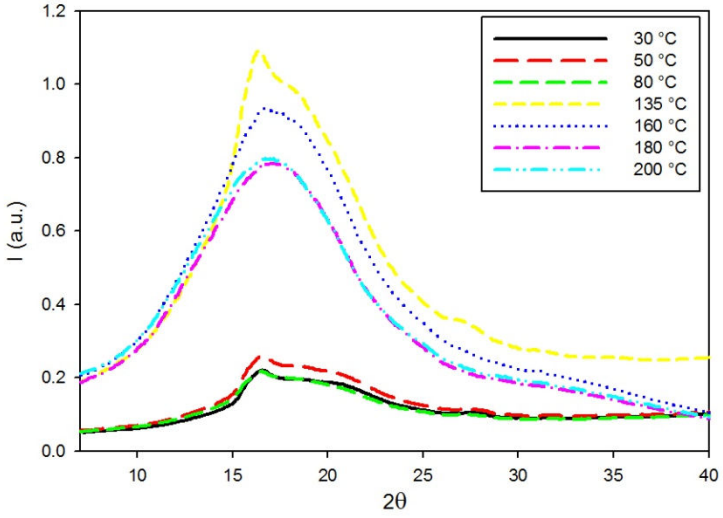

Figure 3.17: WAXD patterns of **0s-30** at various temperatures during heating step-scan.

For the variable temperature WAXD analysis of the **0s-30**, the sample was pressed between two metal discs of which the bottom one was in contact with the heating stage. The sample was heated to increasing temperatures and held isothermally for 30 minutes before subjecting it to the analysis. Figure 3.17 shows the disappearance of the diffraction peak between 160 °C and 180 °C. Also, there is a significant reduction in the peak intensity as the sample is heated from 135 °C to 160 °C. The scattering pattern at 180 °C and 200 °C is caused by the amorphous nature of the copolyester sample. The temperature range of melting for the hard segment crystals significantly overlaps with the T_{II} transition, which confirms that T_{II} transition is involves melting of hard segment crystals.

3.4. Dynamic Mechanical Analysis

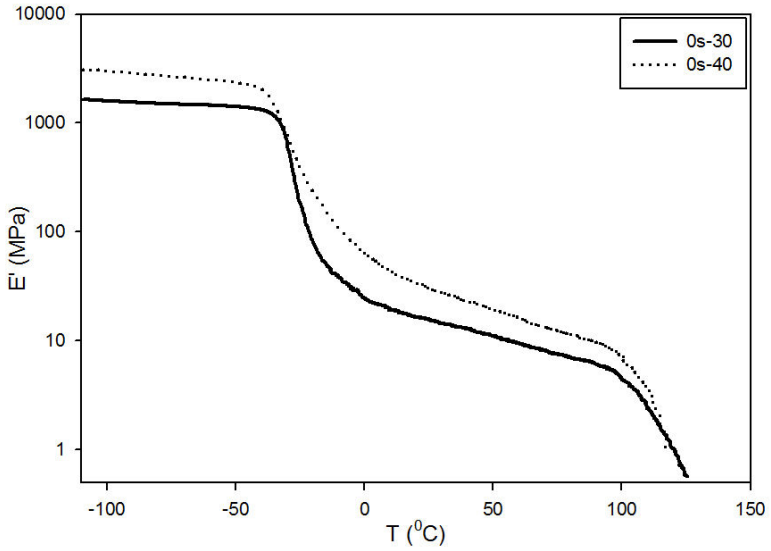

Figure 3.18: Storage modulus spectra of the **0s-30** and **0s-40** annealed at 80 ^{0}C for 24 hours.

The copolyester with higher hard segment content exhibits a higher modulus throughout the temperature range of analysis (Figure 3.18). The modulus decreases by a factor of about 100 as the copolyester goes through the soft segment glass transition. Onset of the decrease is observed at around -40 ^{0}C, which is close to the T_g values reported in the DSC analysis. The second transition begins at about 100 ^{0}C which corresponds to the T_I transition observed in DSC thermograms (local ordering of the hard segments).

3.5. Effect of Annealing on the Morphology and Mechanical Properties of the Copolyesters

3.5.1 Small Angle X-Ray Scattering Analysis

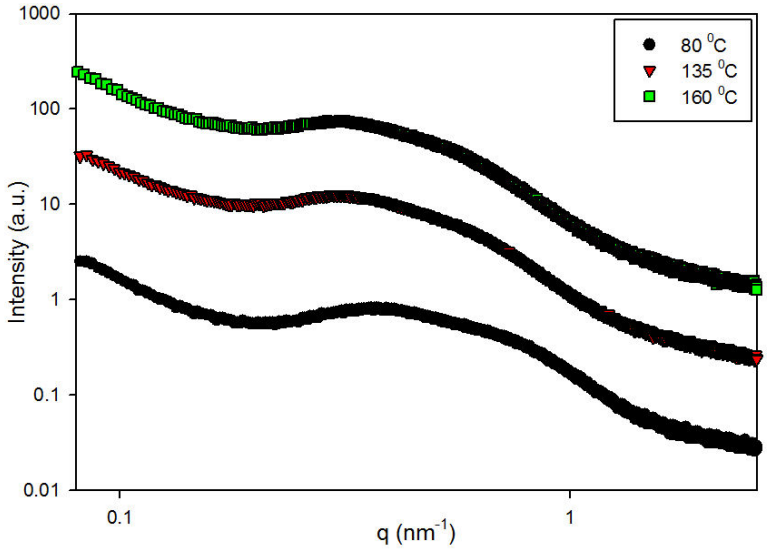

Figure 3.19: SAXS profiles of the **0s-30** annealed at various temperatures. Profiles shifted along Y-axis for clear view.

Annealing shows a significant effect on copolyester morphology. Table 3.2 shows that the local maxima for the Lorentz-corrected SAXS profiles shift to lower values when the copolyester is annealed at higher temperatures. The shift indicates an increased distance between the microphase-separated domains, which can be assigned to a lower number of hard domains in a given volume of the copolyester.

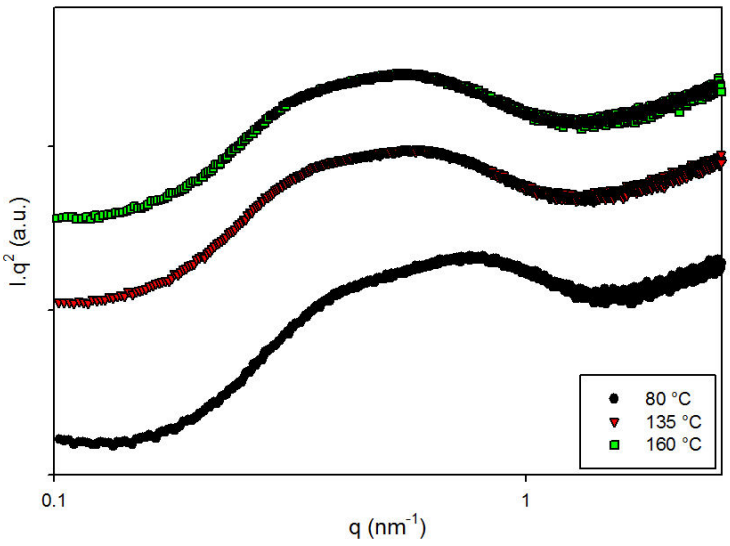

Figure 3.20: Lorentz-corrected SAXS profiles of **0s-30** samples annealed at various temperatures. Profiles shifted along Y-axis for clear view.

Table 3.2 shows the position of the first scattering maximum observed in the Lorentz-corrected SAXS profiles of **0s-30** and **0s-40** samples annealed at various temperatures. The position of the maximum shifts to lower 'q' values with increasing annealing temperatures. Also, **0s-40** samples show the scattering maximum at higher 'q' values compared those observed in **0s-30** samples at the same annealing temperature. The data suggests that the average distance between microphase separated domains is relatively smaller in **0s-40** samples compared to **0s-30** samples. However, considering the broadness of the scattering patterns, these numbers may only be used to observe the changes in the average interdomain spacing.

Table 3.2: Position of scattering maximum for **0s-30** and **0s-40** samples annealed at various temperatures (obtained from Lorentz-corrected SAXS profiles)

Copolyester	Position of Scattering maximum (nm^{-1}) for Annealing Temperature (°C)			Average Interdomain Spacing (nm) for Annealing Temperature (°C)		
	80	**135**	**160**	**80**	**135**	**160**
0s-30	0.39	0.33	0.32	16	19	20
0s-40	0.47	0.41	0.41	13	15	15

3.5.2. Differential Scanning Calorimetry Analysis

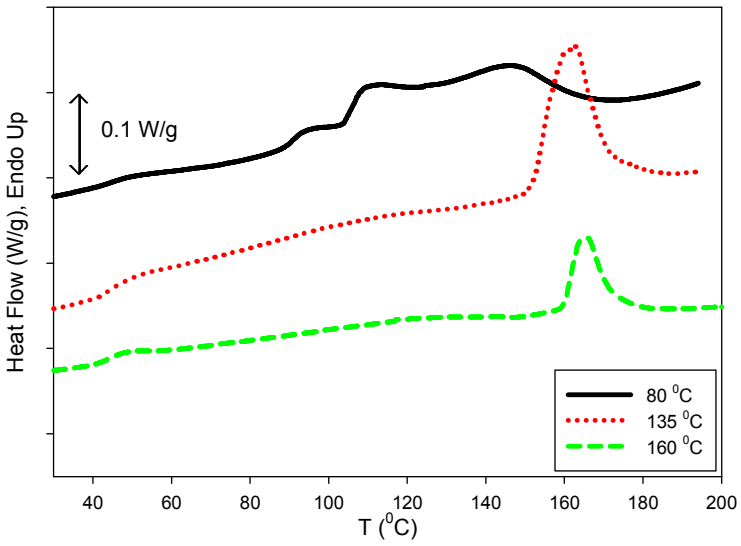

Figure 3.21: DSC thermograms of the **0s-30** annealed at various temperatures. Thermograms shifted along Y-axis.

The DSC thermograms show a shift of the T_{II} transition peak (above 130 °C) with increasing annealing temperature (Figures 3.21 and 3.22). However, the enthalpy change

associated with the transition ΔH_{II} decreases with increasing annealing temperature as reported in Table 3.3.

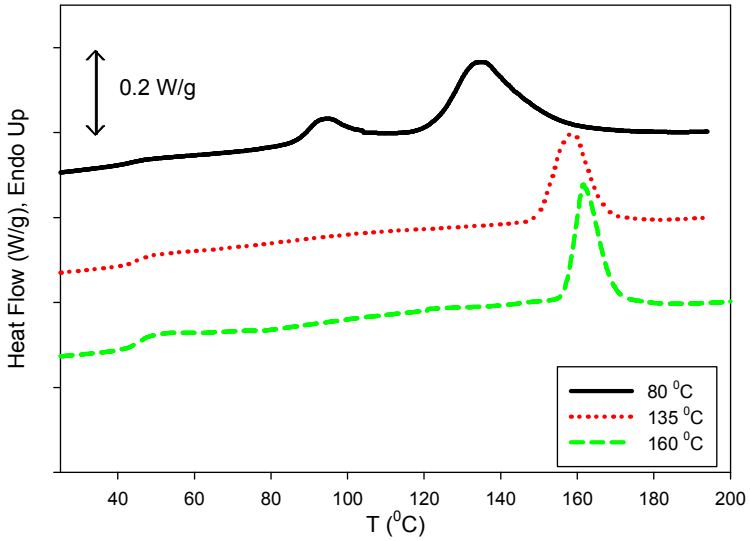

Figure 3.22: DSC thermograms of **0s-40** annealed at various temperatures. Thermograms shifted along Y-axis.

Table 3.3: T_{II} transition temperatures and associated enthalpies of transition (ΔH_{II}) in **0s-30** and **0s-40** annealed at various temperatures.

Copolyester	**T_{II} and Enthalpy of T_{II} transition (ΔH_{II}) for Annealing Temperature (°C)**					
	T_{II} (°C)			**ΔH_{II} (J/g)**		
	80	**135**	**160**	**80**	**135**	**160**
0s-30	145.0 ± 0.8	161.8 ± 0.8	164.8 ±0.1	7.2 ± 0.5	6.2 ± 0.5	4.9 ± 0.3
0s-40	133.5 ± 0.1	157.4 ± 0.4	162.1 ±0.8	10.3 ± 0.3	6.6 ± 0.4	6.4 ± 0.1

The changes in the thermograms of **0s-40** are more pronounced. As annealing temperature increases, the T_{II} transition peak shifts to higher temperatures and becomes sharper. The shift to higher temperatures suggests that the hard segment crystals are better organized. However, the lower values of ΔH_{II} mean that the overall crystallinity in the microphase separated hard domains has decreased. This analysis is in excellent agreement with the SAXS data. The better organized hard segments should exhibit higher electron density contrast with the soft microphase resulting in sharper scattering maxima. Also, as the number of microphase separated domains decrease, the distance between such domains should increase, allowing the scattering maxima to shift to lower scattering vectors.

3.5.3. Dynamic Mechanical Analysis

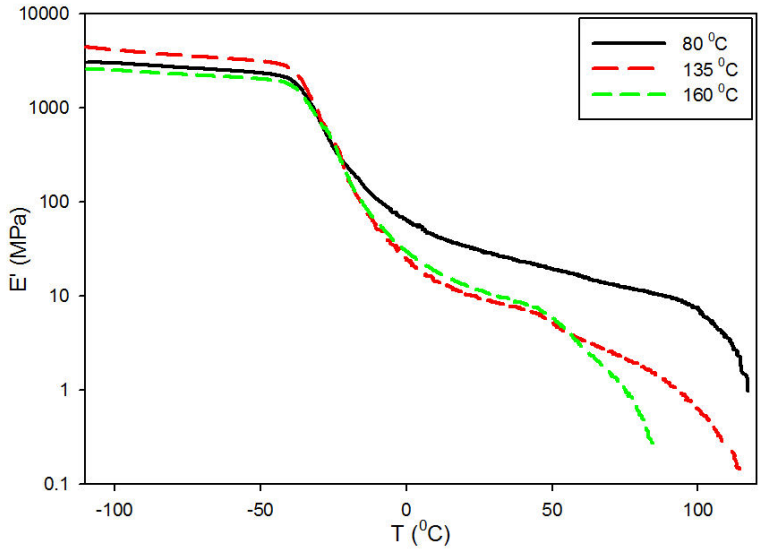

Figure 3.23: Storage modulus spectra of the **0s-40** samples annealed at various temperatures.

The effect of annealing can also be seen with the DMA data of the **0s-40** copolyester (Figure 3.23). The copolyester annealed at 80 ^{0}C shows higher modulus over the rubbery plateau region as compared to the samples annealed at 135 ^{0}C and 160 ^{0}C. A higher modulus indicates

the presence of crosslinks, which consequently suggests higher number of crystalline hard segment domains. Therefore it can be deduced that annealing at high temperatures results in lower number of crystalline hard segment domains. Consequently, the number of physical crosslinks and modulus decrease.

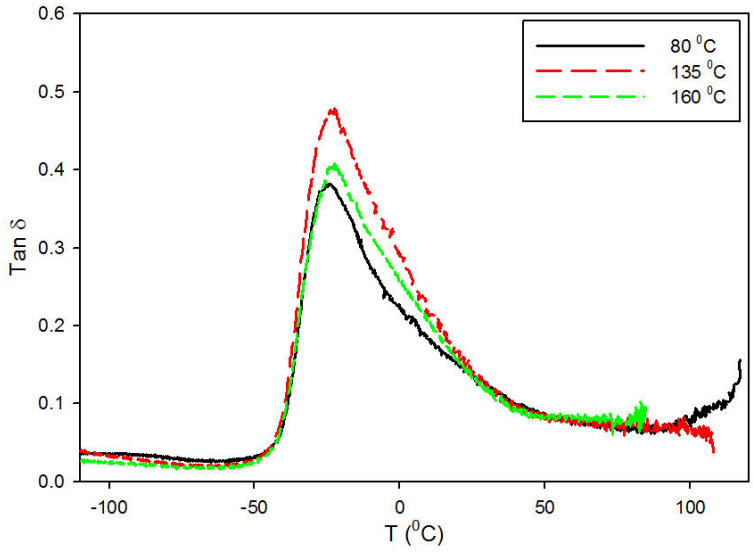

Figure 3.24: Tan delta spectra of the **0s-40** samples annealed at various temperatures.

The peak observed in tan delta spectra of 0s-40 samples (Figure 3.24) corresponds to the glass transition of the soft segments in the copolyester. The peak temperature increases from -26°C to -24 °C as annealing temperature increases from 80 °C to 135 and 160 °C. Also, the glass transition peak becomes broader in samples annealed at 135 and 160 °C, suggesting increased phase-mixing in the copolyester.[52]

3.6. Conclusions

The DSC and X-ray scattering studies led to a significant understanding of the copolyester morphology. The SAXS analysis showed that the copolyesters exhibit a two-phase morphology. The soft segment T_g in the copolyesters is close to that of the pure soft segments, which means that the hard and soft segments are incompatible even though both are of polyester type. The two endothermic transitions, T_I and T_{II}, are identified. T_I is assigned to melting of the local ordering in hard segments. The quench-isothermal analysis shows an increase of about 2°C in the soft segment T_g upon annealing at temperatures close to / higher than T_{II}, which suggest an increased microphase mixing at those temperatures. The hard segments show a small amount of crystallinity but not a highly ordered structure, as indicated by a broad diffraction peak observed in the WAXD analysis. Since the diffraction peak disappears gradually between 135 and 180 °C, the T_{II} transition observed in a similar temperature range in DSC analysis, may involve the melting of crystalline hard segments. The variable temperature SAXS analysis shows decreasing electron density difference between the two microphases in the temperature range of T_{II} transition, which suggests that the melting of hard segment crystals is followed by significant microphase mixing.

Fast scanning calorimetric analysis (heating rates of the order 30,000 K/min) of poly(ethylene terephthalate)[20] and isotactic polystyrene[97] by Schick et al. have provided evidence for the melting-recrystallization-melting process in semicrystalline polymers. The same argument can be applied to the T_I and T_{II} transitions observed in the copolyesters. The copolyesters may also involve melting of crystals during T_I transition, followed by recrystallization and eventually melting during the T_{II} transition. However, the copolyesters are more complex systems since they involve the miscibility of hard and soft segments as well.

Annealing of the copolyesters causes reorganization of hard segments crystals, as observed in DSC analysis. Higher annealing temperatures result in a better ordering of the hard segments, but it also increases miscibility between the two microphases. The X-ray scattering and DSC analyses show that the copolyester with higher hard segment content contains higher number of microphase separated domains. Higher annealing temperatures cause a significant change in the storage modulus of the copolyesters. A lower modulus is observed in the rubbery plateau region as annealing temperature increases, which supports the argument of decreasing number of crystalline hard domains that act as physical crosslinks. This trend suggests that the mechanical properties of the copolyester are dependent on the number of physical crosslinks and not necessarily on the size of or the ordering within the microphase separated domains that act as physical crosslinks.

Chapter 4: Thermal and Morphological Analysis of Sulfonate Containing Segmented Copolyesters

4.1. Introduction

Introduction of ionic groups in the block copolymer chain is an effective route to alter its morphology. The electrostatic interactions within ionic groups significantly affect the mechanical properties as reported in case of copolymers containing carboxyl groups.[98] Several morphological models state that ionic groups in polymers undergo aggregation.[98-100] These ionic aggregates are hydrophilic and can transport ions, while the polymer backbone is usually hydrophobic in nature.[101] Ion containing copolymers have become a potential candidate as ion exchange membranes[101] and also in biomedical applications due to increased compatibility with blood.[102] Hence, it is essential to study the effect of ionic groups on the morphology of the copolyester system under consideration.

Segmented block copolymer such as polyurethanes can contain anions[59] or cations[103] in their polymer backbone. The copolyesters under consideration contain an anion in polymer backbone, sodium cation being the counter-ion. Szymczyk et al.[63] studied the effect of ionic groups on the morphology of polyester-polyether block copolymers and reported that the ionic groups did not have a significant impact on the microphase separation in the copolymer. However, increasing ion content led to decreasing crystallinity if the polyester segments. The current report involves thermal and scattering analysis of sulfonate containing copolyesters, which may lead to understanding of the influence of ionic groups on the microphase separation and crystallinity in the segmented multiblock copolyesters.

4.2. Sulfonated Hard Segment Containing (SHS) Copolyesters

4.2.1 Differential Scanning Calorimetry Analysis

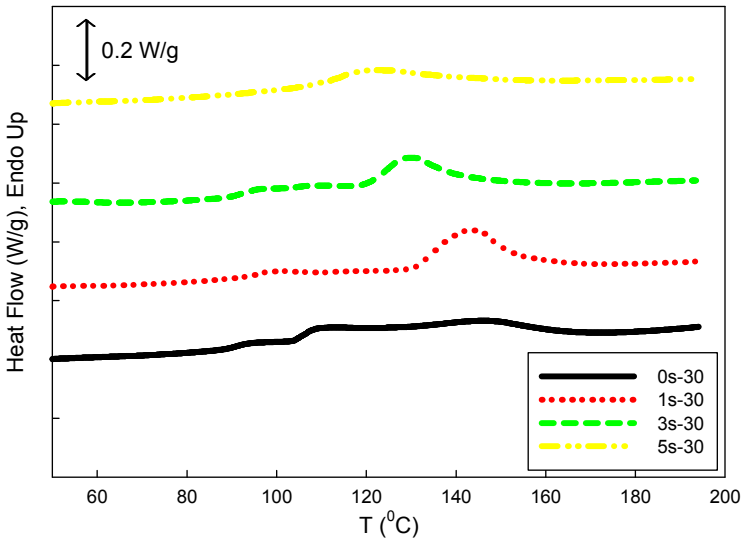

Figure 4.1: DSC thermograms of 30 wt. % HS containing copolyesters annealed at 80 °C. Thermograms shifted along Y-axis.

Similar to the non-sulfonated copolyesters, the SHS copolyesters also show distinct thermal transitions that correspond to the soft segment glass transition, low temperature melting of hard segment crystals (T_I transition) and melting of the hard segment crystals / microphase mixing (T_{II} transition). However, the sulfonated monomer has a significant effect on the enthalpy change associated with the T_{II} transition (ΔH_{II}). As the sulfonate content in the hard segments increases from 0 to 5 mol%, the ΔH_{II} values decrease (Figure 4.13). This decrease implies that the sulfonated hard segments are less ordered than their non-sulfonated analog.

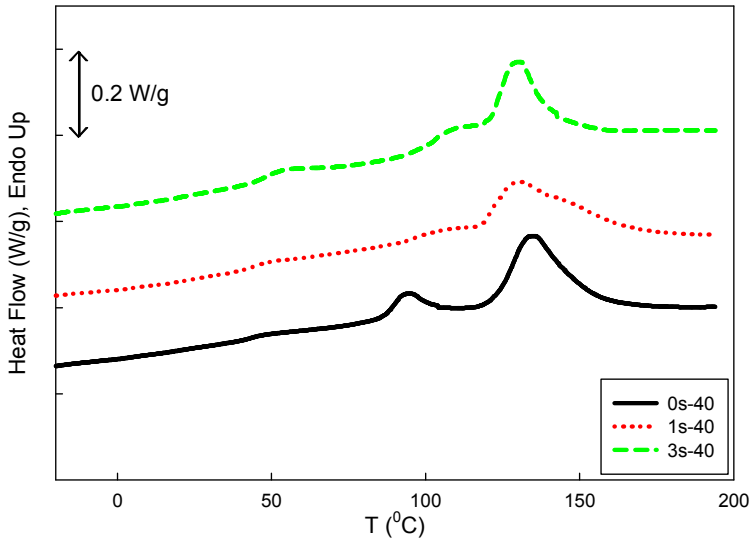

Figure 4.2: DSC thermograms of 40 wt. % hard segment containing copolyesters annealed at 80 °C. Thermograms shifted along Y-axis.

The thermal transitions appear more prominently in the copolyesters containing 40 wt. % hard segments (HS). However, the increasing sulfonate content in this series of copolyesters also leads to similar trends observed in 30 wt. % HS containing copolyesters (Figure 4.14).

4.2.1.1. Quench-isothermal Analysis

In this analysis, the copolyester samples were held at 200 °C for 5 minutes to erase their previous thermal history. Samples were then quenched to various temperatures and held isothermally for 1 hour. Samples were then quickly cooled down to -90 °C, held isothermally for 5 minutes and heated back up to 200 °C at 5°C/min rate.

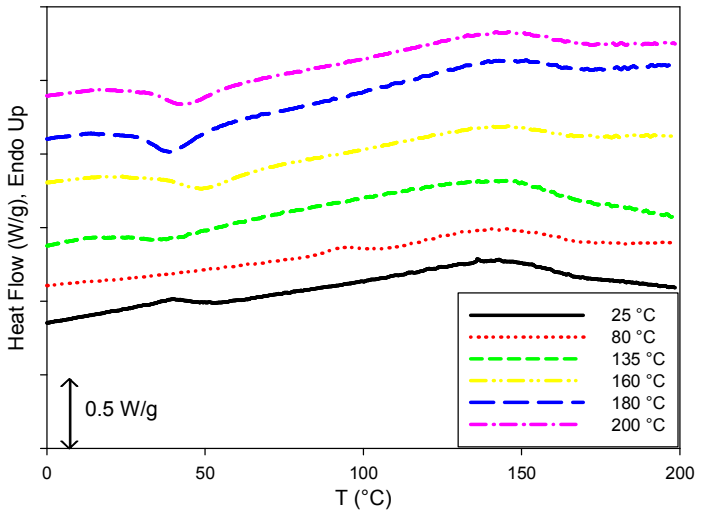

Figure 4.3: Effect of quench temperature on thermal behavior of **1s-30**. Quench temperatures shown in the legend. Thermograms shifted along Y-axis.

The T_I transition peak occurs approximately 20 °C higher than the quench temperature, which confirms the crystallization in the hard segments due to annealing (Figure 4.3). At quench temperatures 135 °C and above, an exotherm appears during the heating scan that corresponds to cold crystallization of hard segments. This data suggests that crystallization and subsequent microphase separation occur during the heating of the copolyester sample.

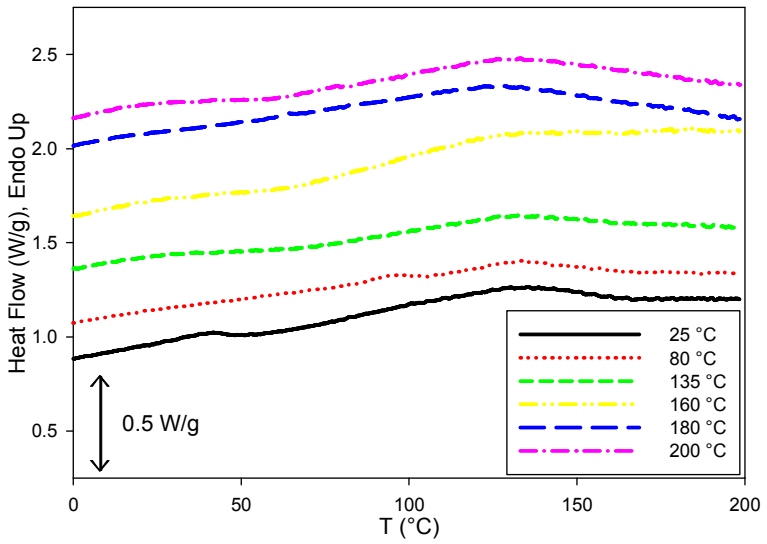

Figure 4.4: Effect of quench temperature on thermal behavior of **5s-30**. Quench temperatures shown in the legend. Thermograms shifted along Y-axis.

At 5 mol % sulfonate content in the hard segments, a weak T_I transition can be seen for the samples quenched to 25 and 80 °C (Figure 4.4). However, in the samples quenched at higher temperatures, an exothermic transition is not observed during the heating scans indicating a lower degree of crystallinity. Also, the T_{II} transition peak becomes broader, which suggests a very weak ordering in the hard segments. Thus, this analysis suggests that the copolyesters with sulfonated hard segments are less ordered compared to their non-sulfonated analogs.

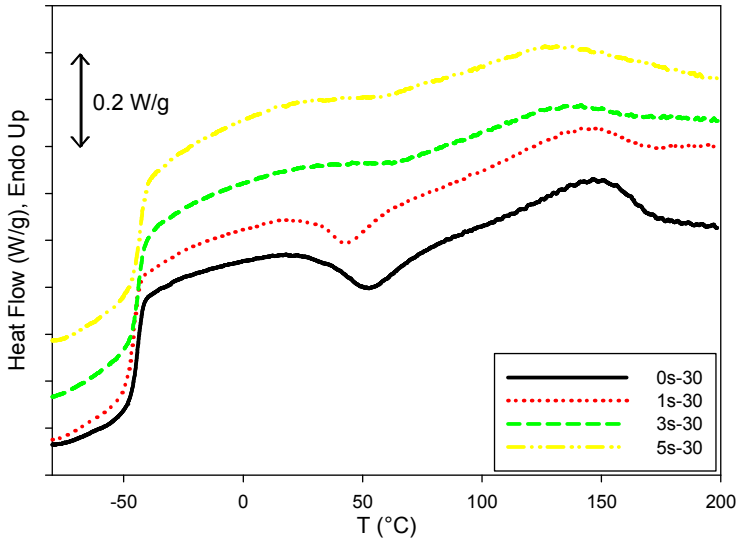

Figure 4.5: Effect of sulfonation in the hard segment on the thermal behavior of 30 wt. % HS containing copolyesters. Samples held isothermally for 1 hour at 200 °C. Thermograms shifted along Y-axis.

In the case of copolyesters containing 30 wt. % hard segments (Figure 4.5) the exothermic transition and the T_{II} transition become progressively weaker with increasing sulfonate content in the hard segments. These results suggest that the sulfonate groups in hard segments act as defects and hamper the ordering of the hard segments. Destruction of the crystallinity may also result in enhanced microphase mixing.

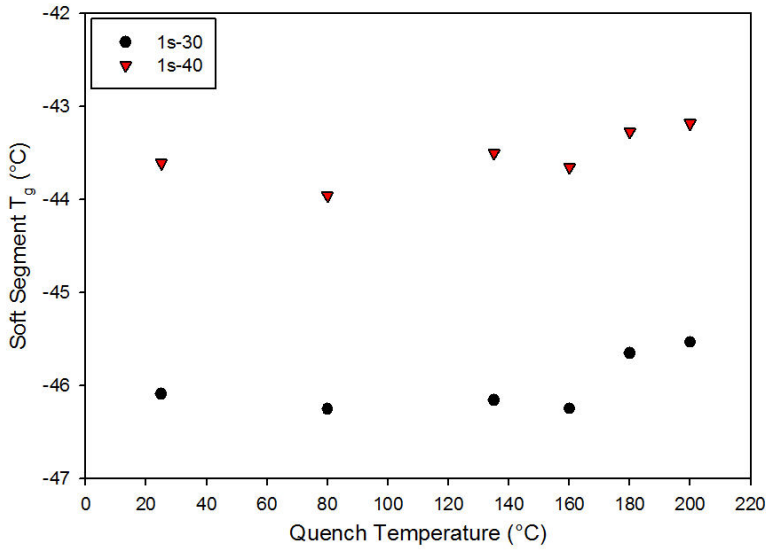

Figure 4.6: Effect of quench temperature on the soft segment T_g of **1s-30** and **1s-40**. (Standard deviation ~1%)

The 40 wt. % hard segment containing polyesters show a higher soft segment T_g for the sulfonated copolyesters as well. The soft segment T_g slightly increases when the quench temperature increases from 80 °C to 200 °C, suggesting microphase mixing occurring between 80 °C and 200 °C. The presence of sulfonate groups in the hard segments also leads to an increased soft segment T_g as seen in Figure 4.7. With the exception of **1s-30**, all of the sulfonated copolyesters show a higher soft segment T_g compared to their non-sulfonated analogs. This data suggests that the sulfonated copolyesters lead to the mixing of more hard segments into the soft microphase, restricting the mobility of the soft segments. At quench temperatures above the T_{II} transition, the sulfonated copolyesters show an increased soft segment T_g, indicating increased microphase mixing.

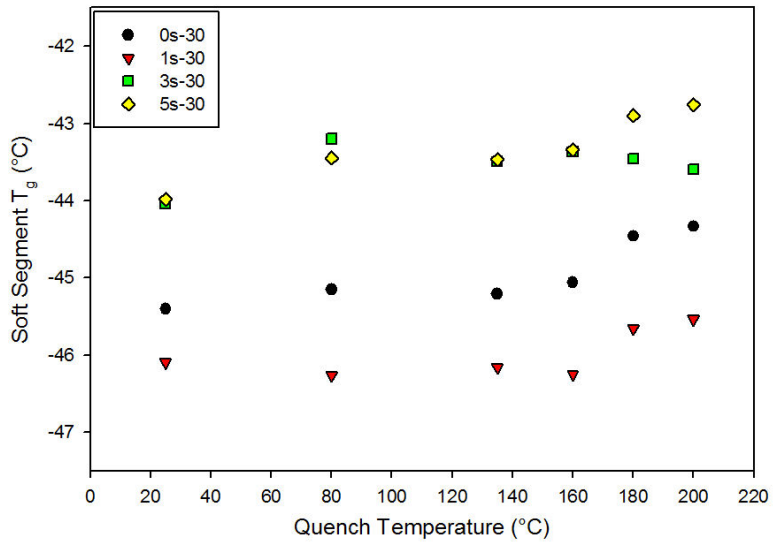

Figure 4.7: Effect of quench temperature and sulfonation in HS of 30 wt. % HS containing copolyesters on soft segment T_g. (Standard deviation ~1%)

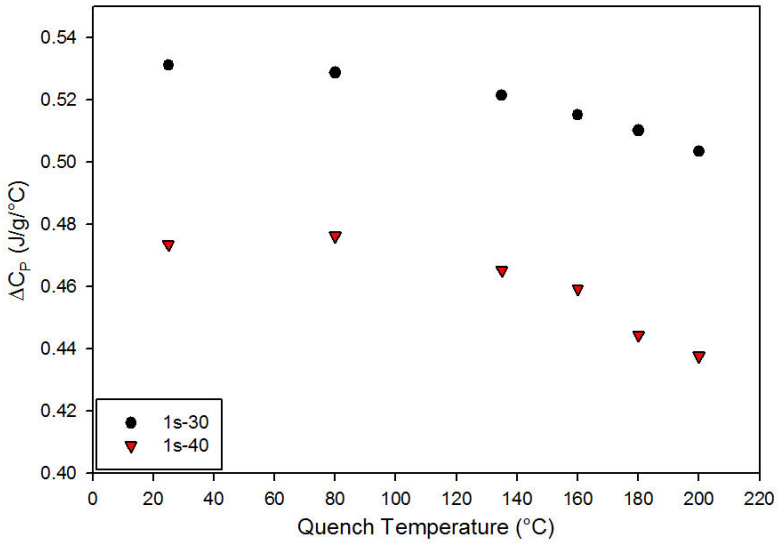

Figure 4.8: Effect of quench temperature on the ΔC_P during soft segment glass transition of **1s-30** and **1s-40**. (Standard deviation ~1%)

Similar to the non-sulfonated copolyesters, the sulfonated copolyesters show lower values of ΔC_P in samples with higher hard segment content. The gradual decrease in the ΔC_P

suggests the increasing extent of microphase mixing throughout the temperature range of analysis.

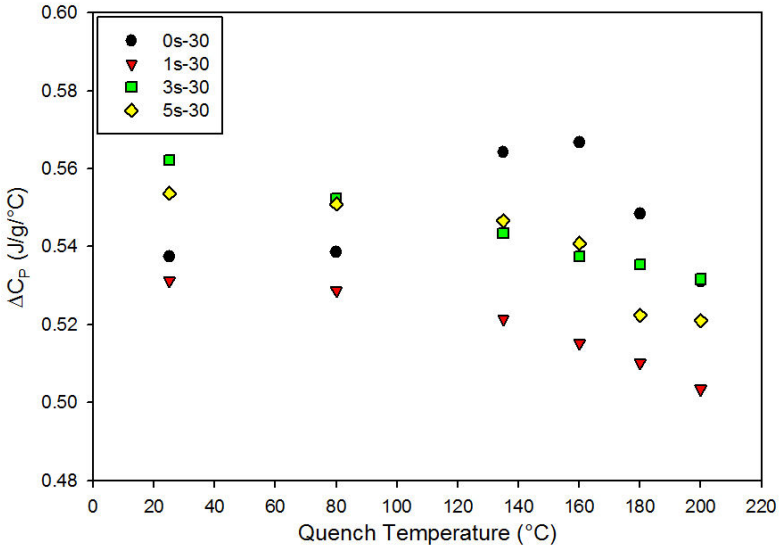

Figure 4.9: Effect of quench temperature, and sulfonation in hard segments, on the ΔC_P during soft segment T_g of 30 wt. % HS containing copolyesters. (Standard deviation ~1%)

Unlike their non-sulfonated counterpart, the sulfonated copolyesters show a gradual decrease in the ΔC_P with increasing quench temperature. However, the ΔC_P values exhibit a more dramatic decrease in samples quenched to temperatures above 135 °C, meaning that a significant microphase mixing takes place above 135 °C.

4.2.2 Small Angle X-Ray Scattering Analysis

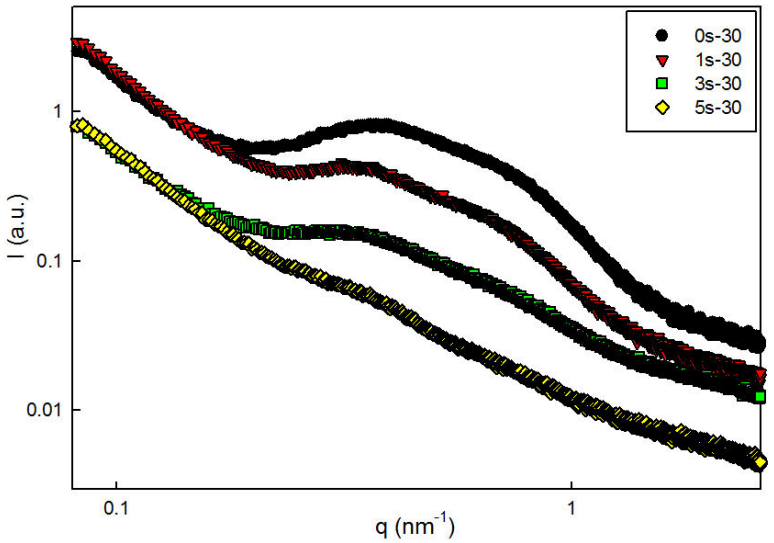

Figure 4.10: Effect of sulfonation in the hard segments on the morphology of 30 wt. % HS containing copolyesters annealed at 80 °C. Scattering profiles shifted along Y-axis.

Figure 4.10 shows the SAXS profiles of non-sulfonated and sulfonated copolyesters, both containing 30 wt. % HS, annealed at 80 °C. The profiles are shifted vertically for a clearer view. The scattering maximum corresponds to the average distance between the microphase-separated hard domains in the copolyesters. The intensity of the maximum is proportional to the electron density difference between the hard and soft microphases. The domains rich with hard segments will exhibit higher electron densities than the soft microphase, contributing toward the intensity of the maximum. The most prominent maximum is observed for **0s-30**. The intensity of maximum decreases as the degree of sulfonation in the hard segments increases. This decrease can be associated with the breaking down of the ordered structure of hard segments due to the presence of the sulfonate groups acting as defects. In the case of **5s-30**, the scattering maximum almost vanishes, suggesting a very weak ordering of the hard segments.

4.2.3. Effect of Annealing on Copolyester morphology

4.2.3.1 Differential Scanning Calorimetry Analysis

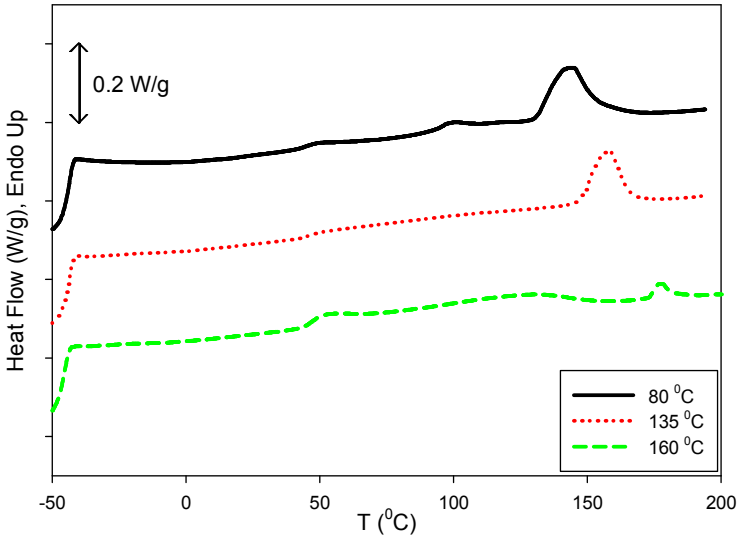

Figure 4.11: Effect of annealing on the thermal behavior of **1s-30**. Thermograms shifted along Y-axis.

Annealing at different temperatures affects the endothermic transitions in the sulfonated copolyesters. A small T_I transition can be seen around 100 °C that occurs due to the crystallinity in the hard segments. With increasing annealing temperatures, this transition merges with the T_{II} transition observed at higher temperatures. These transitions are more prominent in copolyesters with higher hard segment content (**1s-40**) as seen in Figure 4.12.

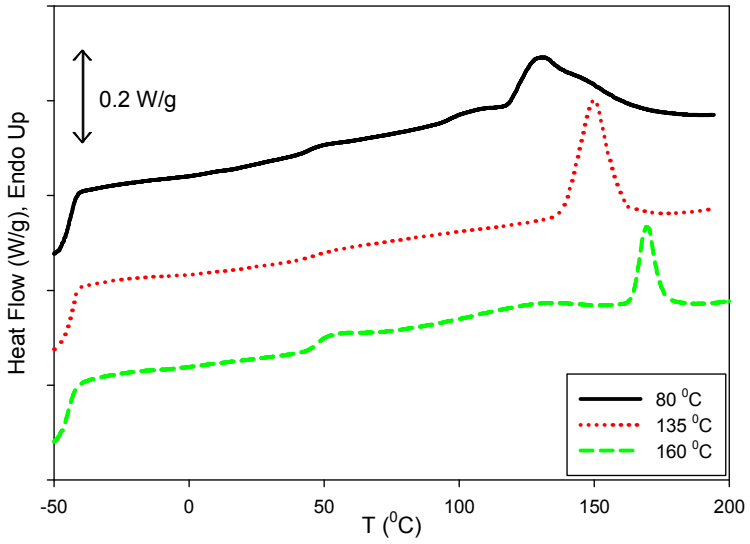

Figure 4.12: Effect of annealing on thermal behavior of **1s-40**. Thermograms shifted along Y-axis.

The thermograms of **1s-40** give a clearer depiction of the impact of the annealing temperature on the thermal behavior of these copolyesters. The increasing annealing temperature shifts the T_{II} transition to higher temperatures, which suggests that the hard segments are well-ordered at higher annealing temperatures. Also, the higher annealing temperatures result in a greater extent of microphase mixing, which effectively reduces the amount of hard segments undergoing the ordering process. Consequently, the enthalpy change associated with the T_{II} transition (ΔH_{II}) decreases. When the annealing temperature overlaps with the T_{II} transition (160 °C), some hard segments crystallize as the temperature starts decreasing after the annealing treatment. These crystals vary in size and their melting appears as a broad transition below the annealing temperature (around 125 °C for **1s-40**). Also, when the samples are cooled down to room temperature after annealing, some hard segments undergo crystallization due to room temperature annealing. Melting of such domains appears as a small endotherm around 50 °C. These two endotherms are prominent in the copolyesters with higher hard segment content

annealed at 160 °C, likely due to the availability of more hard segments for crystallization at lower temperatures.

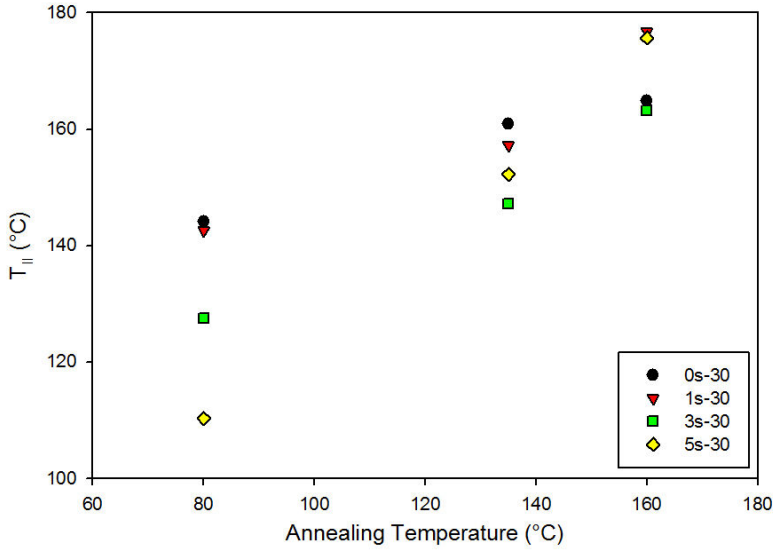

Figure 4.13: Effect of annealing temperature on T_{II} transition of 30 wt. % hard segment containing copolyesters.

The T_{II} transition peak temperature is a measure of the size of the domains that undergo the said transition. For samples annealed at 80 and 135 °C, the peak temperature decreases with increasing sulfonate content in the hard segments, which means that the size of the hard segment crystals decreases with increasing sulfonate content. This data supports the argument that the sulfonated monomer in the hard segments acts as a defect and hampers the long-range ordering.

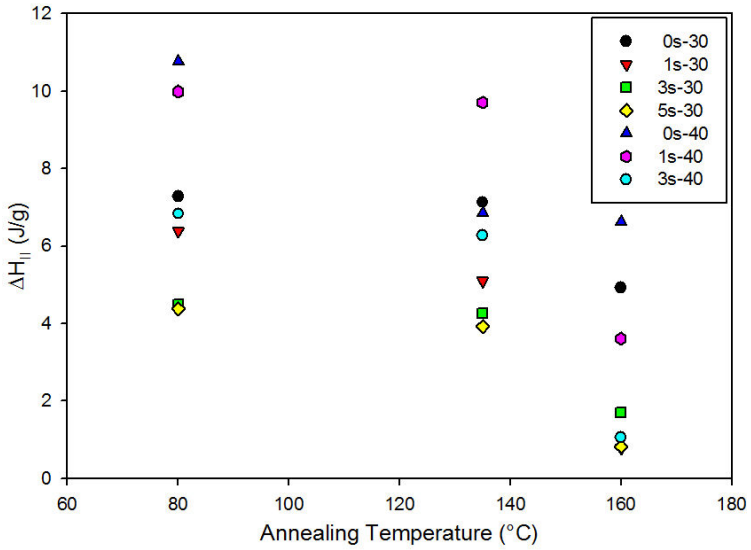

Figure 4.14: Effect of annealing temperature on the enthalpy change during the T_{II} transition (ΔH_{II}) in sulfonated and non-sulfonated copolyesters.

Generally, the copolyesters with higher hard segment content exhibit higher values of ΔH_{II} throughout the temperature range of analysis. The ΔH_{II} values also decrease with increasing levels of sulfonation at a given hard segment content. This suggests that the sulfonate groups not only reduce the size of ordered hard domains, but also reduce the number of hard segments constituting the ordered structure.

4.2.3.2. Small Angle X-ray Scattering Analysis

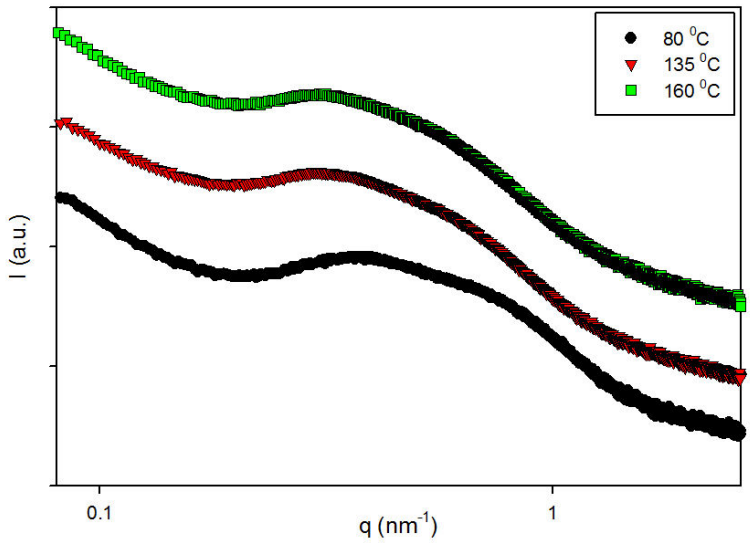

Figure 4.15: Effect of annealing temperatures on the morphology of **1s-30**. Scattering profiles shifted along Y-axis.

SAXS profiles of **1s-30** show a similar trend to that of their non-sulfonated analog. The scattering maximum shifts to lower scattering vectors suggesting an increasing distance between the microphase-separated hard domains. This trend correlates well with the data obtained from thermal analysis. The increasing distance between hard domains can be associated with the decreasing number of hard domains that result from increased microphase mixing at higher annealing temperatures.

4.3. Sulfonated Soft Segment Containing (SSS) Copolyesters

4.3.1 Differential Scanning Calorimetry Analysis

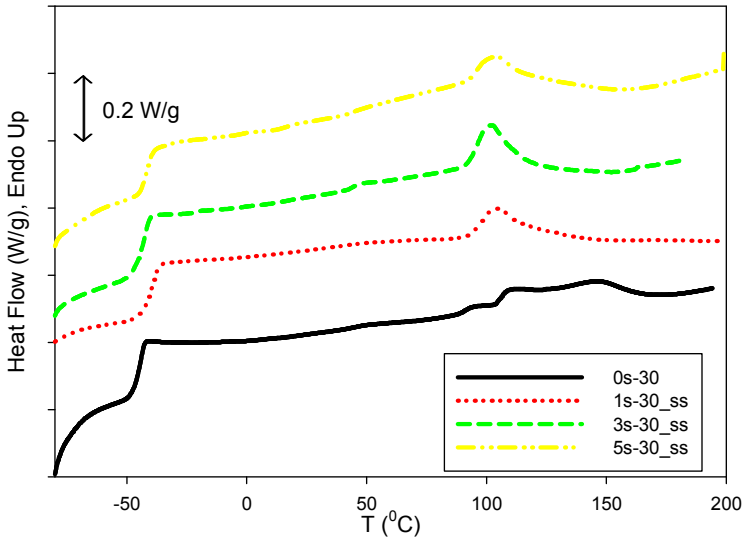

Figure 4.16: DSC thermograms of 30 wt. % hard segment containing SSS copolyesters annealed at 80 °C. Thermograms shifted along Y-axis.

The SSS copolyesters show different thermal behaviors as compared to the sulfonated hard segment containing (SHS) copolyesters. The most important difference is the absence of the T_{II} transition, which corresponds to the melting of crystalline hard segments. Only the T_I transition appears in SSS copolyesters, approximately 20 °C above the annealing temperature. Also, the enthalpy change associated with T_I becomes more significant with increasing sulfonate content.

In the case of SHS copolyesters, the sulfonate groups present in the hard segments act as defects and reduce the crystallinity. In SSS copolyesters, the ionic groups are not expected to interfere with the hard segment crystallization, but the DSC data does not support this argument.

It is clear from the Figure 4.16 that even though the ionic groups are present in the soft segments, the copolyester morphology is considerably altered.

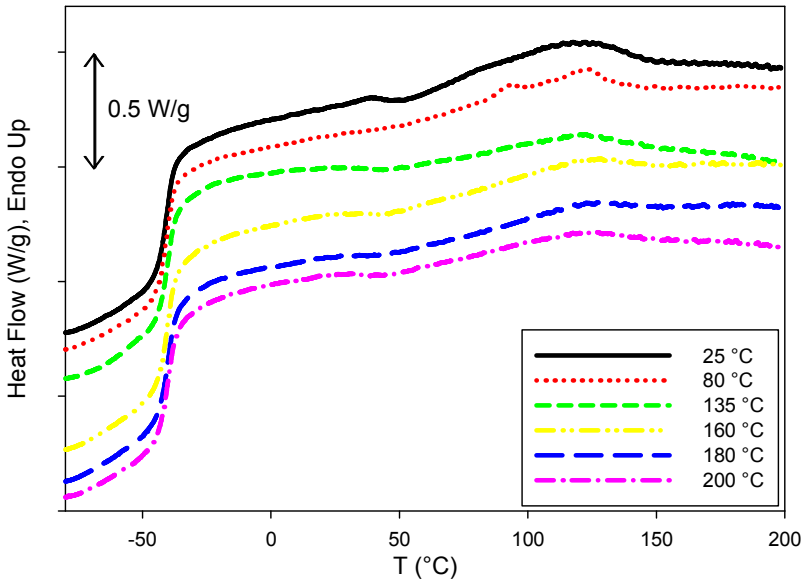

Figure 4.17: Effect of quench temperature on thermal behavior of **1s-30_ss**. Quench temperatures shown in the legend. Thermograms shifted along Y-axis.

The quench-isothermal analysis shows a broad T_{II} transition, which is absent in DSC thermograms of solution cast, 80 °C annealed samples. The broadness of this transition suggests that the melting of hard segment crystals in these copolyesters takes place over a very broad temperature range, which overlaps with the T_I transition in solution cast copolyesters.

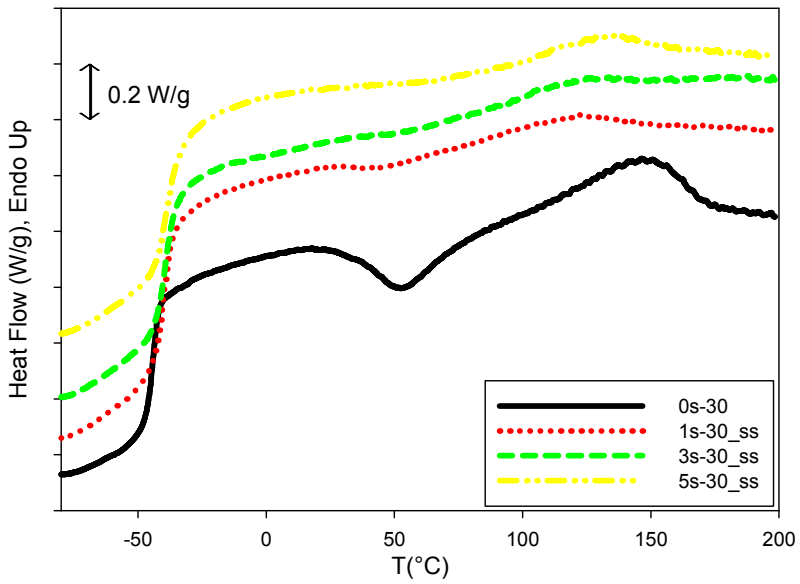

Figure 4.18: Effect of sulfonation in soft segment on thermal behavior of 30 wt. % HS containing copolyesters. Samples held isothermally for 1 hour at 200 °C before quenching to -90 °C. Thermograms shifted along Y-axis.

The sulfonated copolyesters quenched from 200 °C to sub-ambient temperatures show a much weaker exothermic transition that corresponds to cold crystallization of the hard segments (Figure 4.18). In case of **3s-30_ss** and **5s-30_ss**, this transition in negligible. Also, the T_{II} transition is very weak, suggesting a much lower degree of crystallinity in hard segments.

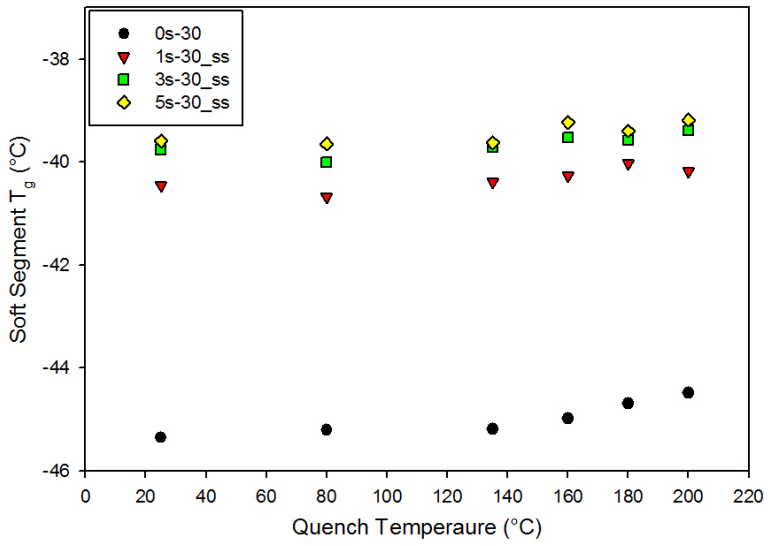

Figure 4.19: Effect of quench temperature and sulfonation in the soft segment, on the soft segment T_g of 30 wt. % HS containing copolyesters. (Standard deviation ~1%)

All sulfonated copolyesters show a significantly higher soft segment T_g than their non-sulfonated analogs (Figure 4.19). Copolyesters containing 3 and 5 mol % sulfonated soft segments exhibit a higher T_g than the 1 mol % sulfonated soft segment analog. This data suggests that the sulfonate groups restrict the mobility of the soft segment either by electrostatic interactions or increased mixing of hard segments in the soft microphase. Samples quenched at 135 °C and above show a slightly higher T_g for all the copolyesters, suggesting increased microphase mixing.

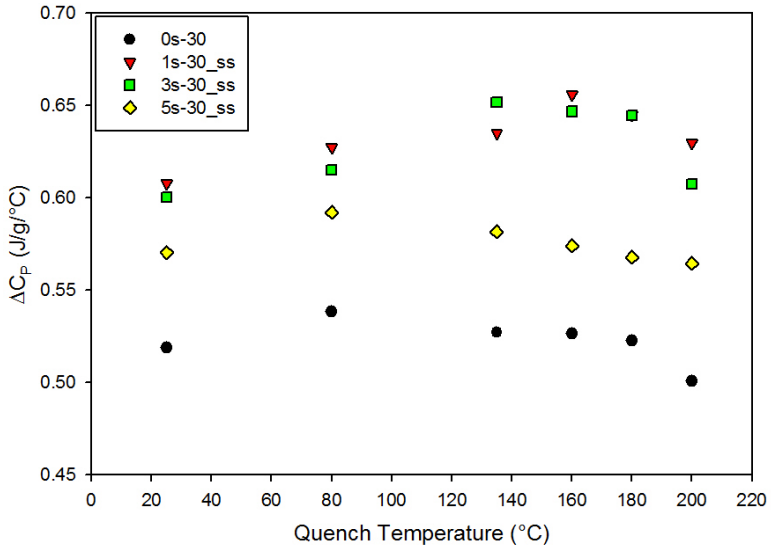

Figure 4.20: Effect of quench temperature and sulfonation in soft segments, on the ΔC_P during soft segment glass transition in 30 wt. % HS containing copolyesters. (Standard deviation ~3%)

The sulfonated copolyesters show a gradual decrease in the ΔC_P during the soft segment glass transition when quenched at 135 °C and above. Figure 4.18 shows that the T_{II} transition peak is around 125 °C, thus samples quenched above 125 °C should yield lower ΔC_P values. The ΔC_P values continue to decrease above 135 °C, which implies that, the microphase mixing is not complete at given temperatures.

4.3.2. Small Angle X-ray Scattering Analysis

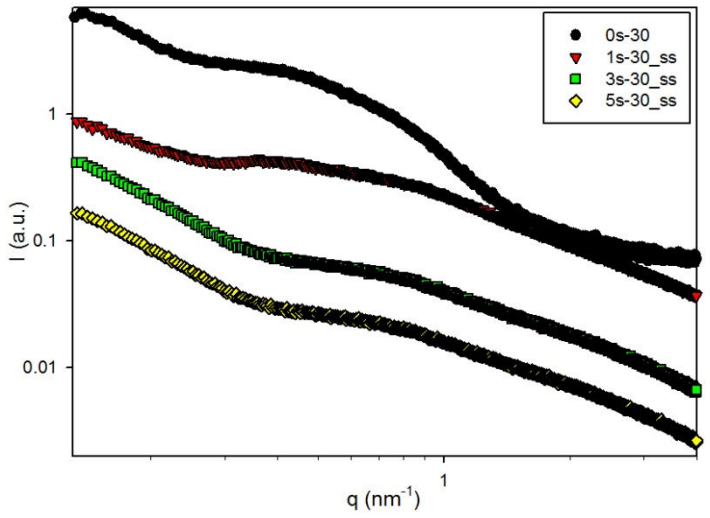

Figure 4.21: Effect of sulfonation in soft segments on the morphology of 30 wt. % hard segment containing copolyesters annealed at 80 °C for 24 hours. Profiles shifted along Y-axis.

The location of the sulfonate groups within the various polyesters shows a significant effect on the copolyester morphology. The sulfonate groups present in hard segments disrupt the order in hard segments as reported previously. At 5 mol% sulfonate content, the disruption of ordering is so severe that it results in significant reduction of the scattering peak intensity. In the case of SSS copolyesters as well, the hard segments lose their ordered structure. The broadness of the scattering peak suggests a wide distribution of distances between microphase separated domains. For SSS copolyesters, this distribution appears shifted toward higher scattering vectors compared to the SHS copolyesters. This shift indicates that the average distance between microphase separated domains is reduced for SSS copolyesters. However, the intensity of the scattering peak is severely reduced in case of SSS copolyesters, suggesting enhanced microphase mixing.

4.4. Effect of Annealing on SSS Copolyester Morphology

4.4.1. Differential Scanning Calorimetry Analysis

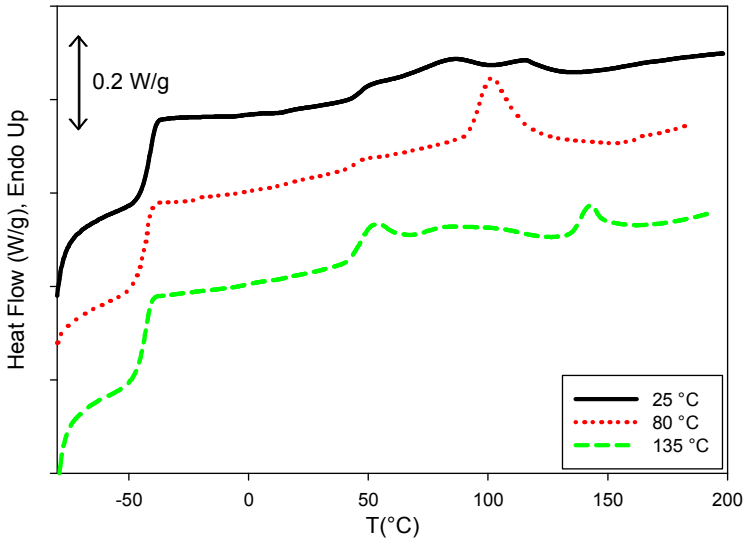

Figure 4.22: Effect of annealing on thermal behavior of **3s-30_ss**. Thermograms shifted along Y-axis.

Similar to the SHS copolyesters, the SSS copolyesters show a gradual shift of the T_I transition peak to higher temperatures with increasing annealing temperatures. As the annealing temperature increases, melting of crystalline hard segments prevails over their reorganization. In the case of **1s-30** being annealed at 160 °C, smaller sized hard domains develop in a broad endotherm that is observed from approximately 60 °C to 130 °C. The endotherm around 50 °C appears most significantly in samples annealed at 160 °C. Since this peak corresponds to the melting of hard segment crystals formed during room temperature annealing, it can be concluded that the hard segments unable to crystallize at high annealing temperatures form crystals at lower temperatures.

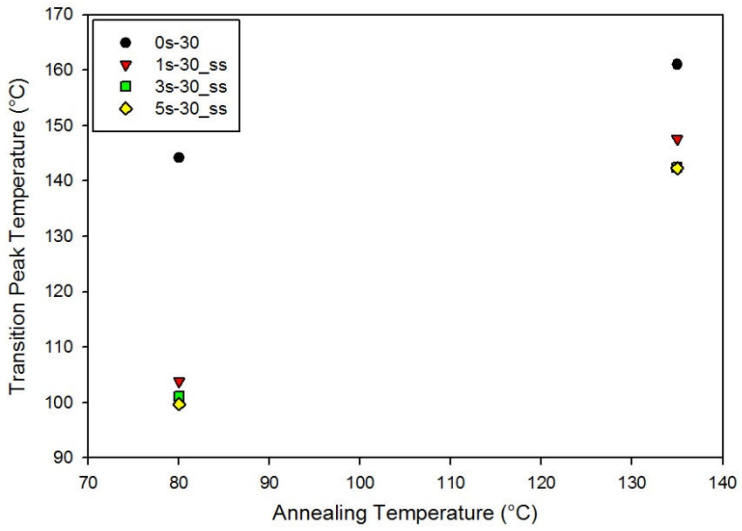

Figure 4.23: Effect of annealing temperature on the T_I transition temperature of 30 wt. % hard segment containing copolyesters.

All SSS copolyester samples show a shift of T_I transition to higher temperatures with increasing annealing temperatures. Also, the melting transition appears at much lower temperatures in SSS copolyesters compared to their non-sulfonated analogs. This trend suggests that the sulfonate groups, even though present in the soft segments, significantly reduced the hard segment crystallinity. The enthalpy change associated with the T_I transition (ΔH_{tr}) decreases with the increasing sulfonate content in the soft segments, as seen in Figure 4.24. These results also suggest that the increasing sulfonation of soft segments leads to destruction of the crystallinity in the hard segments.

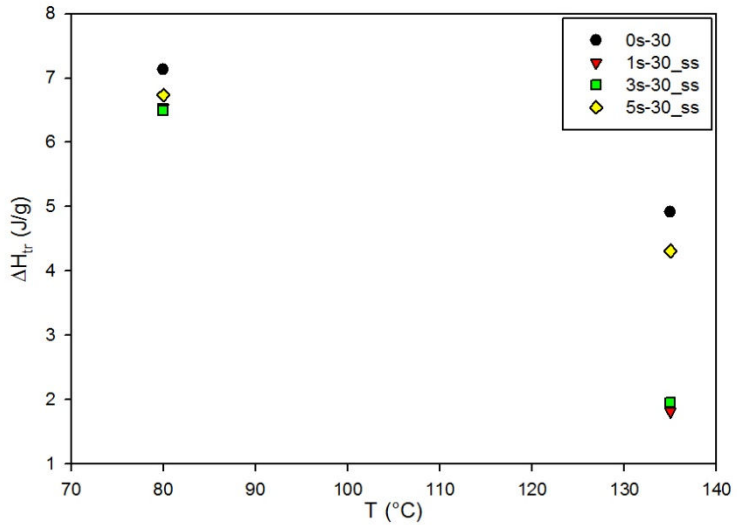

Figure 4.24: Effect of annealing temperature on the ΔH_{tr} in 30 wt. % hard segment containing SSS copolyesters.

4.4.2. Small Angle X-Ray Scattering Analysis

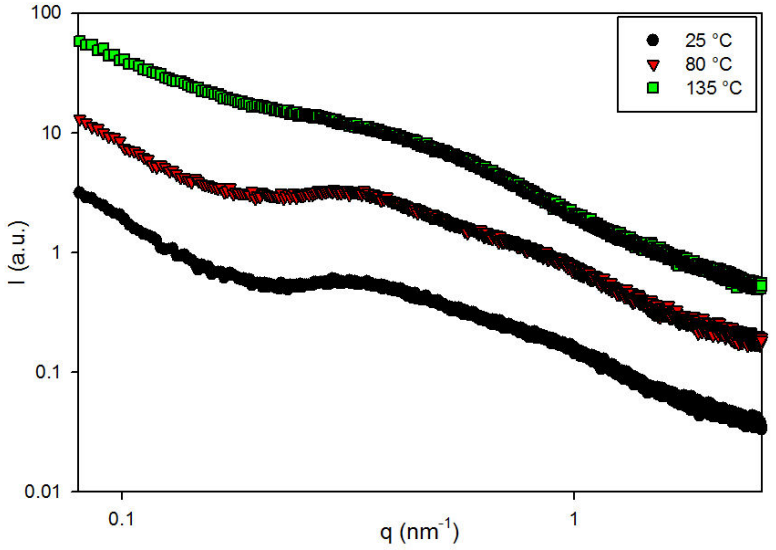

Figure 4.25: Effect of annealing temperature on the morphology of **3s-30_ss**. Scattering profiles shifted along Y-axis.

The **3s-30_ss** sample shows similar scattering profiles when annealed at 25 and 80 °C. However, when annealed at 135 °C, significant morphological changes take place in the sample,

which results in a distinct scattering profile. In the case of copolyester annealed at 135 °C, the scattering maximum appears diminished compared to the samples annealed at lower temperatures. This behavior is an indication of destruction of crystallinity and microphase mixing.

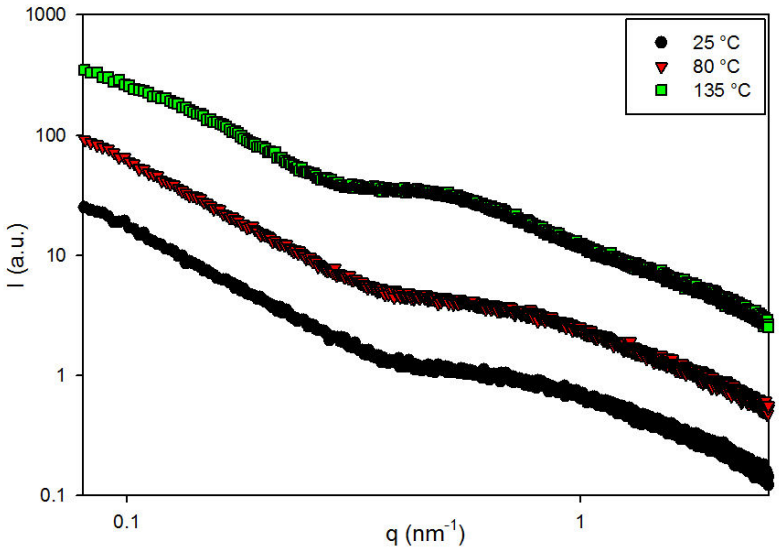

Figure 4.26: Effect of annealing temperature on the morphology of **5s-30_ss**. Scattering profiles shifted along Y-axis.

5s-30_ss also undergoes a significant morphological change when annealed at 135 °C. However, there is no significant loss of microphase-separated domains as observed in **3s-30_ss**. Instead there is a development of a scattering maximum at lower 'q' values. This suggests that the microphase-separated domains exist but the average distance between them has increased at higher annealing temperatures.

4.5. Conclusions

The presence of ionic groups has a significant effect on the thermal behavior and morphology of all the copolyesters studied in this investigation. Not only the amount of ionic groups, but also their occurrence in either the hard or soft microphase considerably changes the morphology. The feature most significantly affected by the sulfonate groups is the crystallinity of the hard segments. In the case of sulfonated hard segments, the sulfonated monomer (Na-SIP) acts as a defect and restricts the organization of hard segments. However, copolyesters with sulfonated groups present in the soft segments also showed diminished hard segment crystallinity. These results suggest that the Na-SIP has a much greater affinity toward the hard segments. SAXS profiles of the copolyesters do not show a peak corresponding to the ionic aggregation, so it is more likely that the Na-SIP units primarily act as physical defects. Furthermore, electrostatic interactions between the ionic groups may not necessarily contribute toward the loss of crystallinity in the hard segments.

The soft segment T_g obtained for the copolyesters during the quench-isothermal analysis does not show a large increase over the entire temperature range of analysis, especially when the quench temperature is near or above the T_{II} transition. This means that presence of the hard segments in the soft microphase does not significantly affect the mobility of the soft segments. However, introduction of the sulfonate groups in either the hard or soft segments causes an increase in the soft segment T_g. Samples with sulfonate containing soft segments show relatively higher soft segment T_g than the samples containing sulfonated hard segments. These results lead to the conclusion that the sulfonate (ionic) groups restrict the mobility of the soft segments. Since sulfonate groups interact with both, hard and soft segments, they act as compatibilizers and promote microphase mixing.

Annealing of the sulfonated copolyesters generally leads to reduced crystallinity in hard segments and increased microphase mixing, which would result in the loss of mechanical properties. Soft segments sulfonated copolyesters in general, are less crystalline than hard segment sulfonated copolyesters, and show further reduction in crystallinity after annealing at higher temperatures. However, at 5 mol% sulfonated monomer content in soft segments, the copolyester sample shows different behavior as observed in the SAXS analysis.

Chapter 5: Future Work

5.1. Quantitative SAXS Analysis

This study has utilized the thermal and scattering analytical techniques to provide a base for the further morphological and mechanical analysis by establishing the factors that lead to microphase mixing. However, the impact of the sulfonate groups on the copolyester morphology is still not clear. The quantitative SAXS analysis may help to answer this question. The Porod analysis performed with suitable corrections to the scattering data can lead to estimation of the inhomogeneity length of microphase-separated domains and the interfacial thickness. These parameters are a measure of the structure of microphase separated domains and the degree of microphase mixing respectively. The background scattering intensity (I_b) and Porod's constant (K) for each sample will be calculated by following the procedure described by Verma et al.(Figure 5.1)[104]

Determination of the inhomogeneity length and interfacial thickness for the copolyesters annealed at various temperatures can also provide further detailed information about the changes in the morphology due to annealing. This study will be particularly interesting for **5s-30_ss** as its annealing at 80 °C and 135 °C yields different scattering patterns.

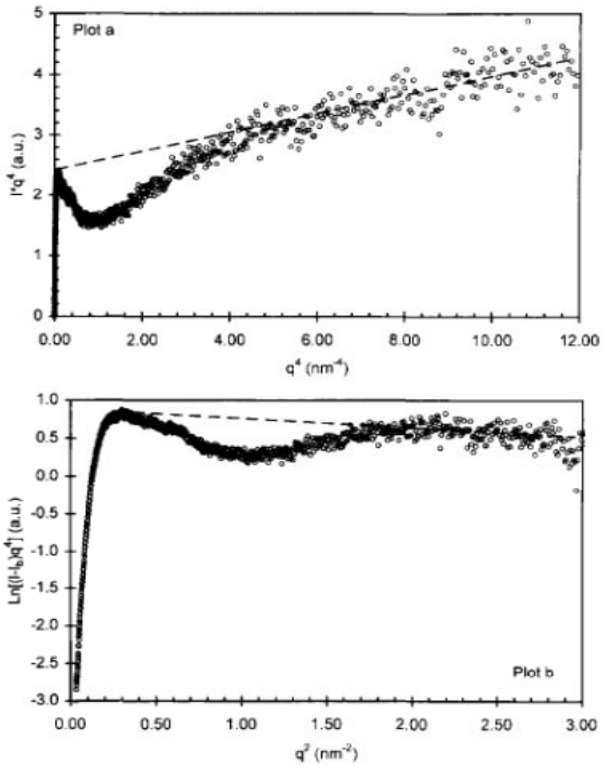

Figure 5.1: (a) In a plot of $I.q^4$ versus q^4, K is calculated as the Y-intercept and I_b is the slope of the straight line. (b) In a plot of $\ln[(I-I_b).q^4]$ versus q^2, the negative slope of the line is the σ^2 (σ = interfacial thickness) and the Y-intercept is the natural log of the refined Porod's constant (K).[104] Reprinted with permission from Verma, R. K.; Velikov, V.; Kander, R. G.; Marand, H.; Chu, B.; Hsiao, B. S., SAXS studies of lamellar level morphological changes during crystallization and melting in PEEK. *Polymer* **1996,** *37* (24), 5357-5365. Copyright 1996. American Chemical Society.

5.2. Dynamic Mechanical Analysis of Copolyesters

The effect of morphological changes, due to ionic groups and annealing processes, on the mechanical properties also needs to be studied. Presence of ionic groups generally leads to increase in the rubbery plateau modulus observed during dynamic mechanical analysis of block copolymers. (Figure 5.2)[105]

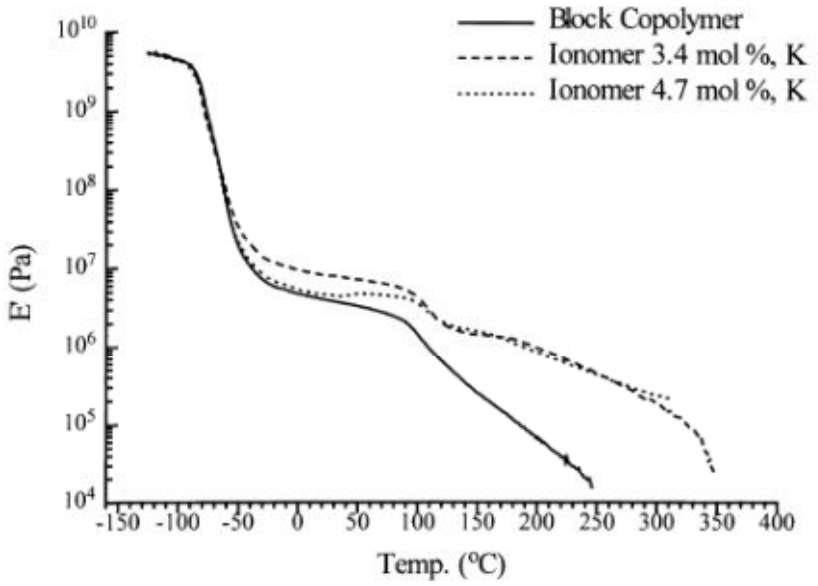

Figure 5.2.: Effect of sulfonate content (in polystyrene block) on the storage modulus of 25.5 wt. % polystyrene containing poly(styrene-b-isobutylene-b-styrene) block copolymers.[105] Reprinted with permission from Storey, R. F.; Baugh, D. W., Poly(styrene-b-isobutylene-b-styrene) block copolymers produced by living cationic polymerization. Part III. Dynamic mechanical and tensile properties of block copolymers and ionomers therefrom. *Polymer* **2001,** *42* (6), 2321-2330. Copyright 2001. American Chemical Society.

A detailed stress-strain analysis and dynamic mechanical analysis of non-sulfonated and sulfonated copolyesters annealed at different temperatures will lead to understanding of the influence of ion content and processing conditions on the morphology and dynamic mechanical behavior of copolyesters.

5.3. Time Dependence of the Evolution of Mechanical Properties

A crucial factor which needs to be given attention to is the evolution of the copolyester morphology as a function of time. Wilkes et al.[24,27,28,73-79] have performed a number of studies on the kinetics of microphase separation in polyurethanes and corresponding changes in their thermal and mechanical properties. It was observed that the Young's modulus of a polyurethane increased with time following the annealing treatment (Figure 5.3).[78]

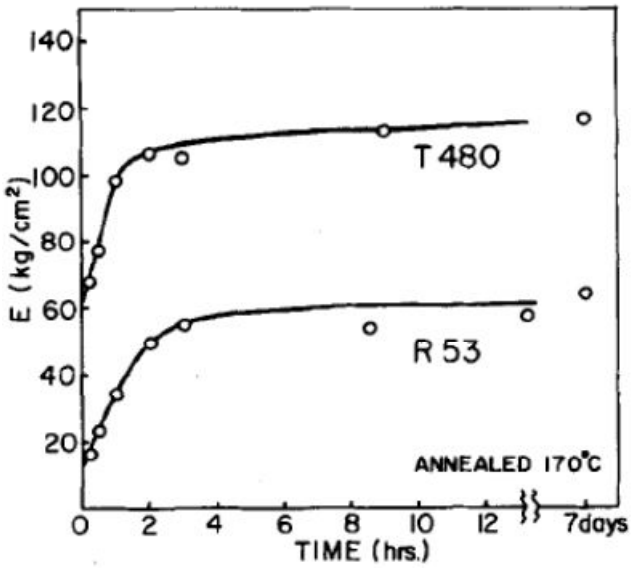

Figure 5.3: Effect of time following the annealing treatment, on the Young's modulus (E) of 4,4'-diphenylmethane diisocyanate based polyurethanes.[78] Reprinted with permission from Wilkes, G. L.; Wildnauer, R., Kinetic behavior of the thermal and mechanical properties of segmented urethanes. *Journal of Applied Physics* **1975,** *46* (10), 4148-4152. Copyright 1975. American Institute of Physics.

A detailed stress-strain analysis of the ion containing copolyesters will lead to understanding of the effect of ionic groups and annealing temperature on the microphase separation and subsequently, on copolyesters' Young's modulus, as a function of post-annealing time.

References

(1) Louie, J. S.; Pinnau, I.; Ciobanu, I.; Ishida, K. P.; Ng, A.; Reinhard, M. *Journal of Membrane Science* **2006**, *280*, 762.

(2) Spontak, R. J.; Patel, N. P. *Current Opinion in Colloid & Interface Science* **2000**, *5*, 333.

(3) Fasolka, M. J.; Mayes, A. M. *Annual Review of Materials Research* **2001**, *31*, 323.

(4) Brown, K.; Hooker, J. C.; Creton, C. *Macromolecular Materials and Engineering* **2002**, *287*, 163.

(5) Bonart, R.; Müller, E. H. *Journal of Macromolecular Science, Part B* **1974**, *10*, 177.

(6) Matsuo, M.; Ueno, T.; Horino, H.; Chujyo, S.; Asai, H. *Polymer* **1968**, *9*, 425.

(7) Cella, R. J. *Journal of Polymer Science: Polymer Symposia* **1973**, *42*, 727.

(8) Raquez, J. M.; Deléglise, M.; Lacrampe, M. F.; Krawczak, P. *Progress in Polymer Science* **2010**, *35*, 487.

(9) Williams, C. K.; Hillmyer, M. A. *Polymer Reviews* **2008**, *48*, 1.

(10) Petrović, Z. S. *Polymer Reviews* **2008**, *48*, 109.

(11) Wang, X.; Xie, X.; Cai, C.; Rytting, E.; Steele, T.; Kissel, T. *Macromolecules* **2008**, *41*, 2791.

(12) Wanamaker, C. L.; O'Leary, L. E.; Lynd, N. A.; Hillmyer, M. A.; Tolman, W. B. *Biomacromolecules* **2007**, *8*, 3634.

(13) Laity, P. R.; Taylor, J. E.; Wong, S. S.; Khunkamchoo, P.; Cable, M.; Andrews, G. T.; Johnson, A. F.; Cameron, R. E. *Journal of Applied Polymer Science* **2006**, *100*, 779.

(14) *Thermal Characterization of Polymeric Materials*; 2 ed.; Academic Press Limited: San Diego, 1997; Vol. 1.

(15) *Multiphase Polymers*; AMERICAN CHEMICAL SOCIETY, 1979; Vol. 176.

(16) Camberlin, Y.; Pascault, J. P. *Journal of Polymer Science: Polymer Chemistry Edition* **1983**, *21*, 415.

(17) Seymour, R. W.; Cooper, S. L. *Macromolecules* **1973**, *6*, 48.

(18) Hesketh, T. R.; Van Bogart, J. W. C.; Cooper, S. L. *Polymer Engineering & Science* **1980**, *20*, 190.

(19) Castles, J. L.; Vallance, M. A.; McKenna, J. M.; Cooper, S. L. *Journal of Polymer Science: Polymer Physics Edition* **1985**, *23*, 2119.

(20) Minakov, A. A.; Mordvintsev, D. A.; Schick, C. *Faraday Discussions* **2005**, *128*, 261.

(21) Chu, B.; Hsiao, B. S. *Chemical Reviews* **2001**, *101*, 1727.

(22) Blackwell, J.; Gardner, K. H. *Polymer* **1979**, *20*, 13.

(23) Gardner, K. H.; Blackwell, J. *Acta Crystallographica Section B* **1980**, *36*, 1972.

(24) Chang, Y.-J. P.; Wilkes, G. L. *Journal of Polymer Science: Polymer Physics Edition* **1975**, *13*, 455.

(25) Briber, R. M.; Thomas, E. L. *Journal of Macromolecular Science, Part B* **1983**, *22*, 509.

(26) Paik Sung, C. S.; Hu, C. B.; Wu, C. S. *Macromolecules* **1980**, *13*, 111.

(27) Tyagi, D.; McGrath, J. E.; Wilkes, G. L. *Polymer Engineering & Science* **1986**, *26*, 1371.

(28) Abouzahr, S.; Wilkes, G. L.; Ophir, Z. *Polymer* **1982**, *23*, 1077.

(29) Koberstein, J. T.; Morra, B.; Stein, R. S. *Journal of Applied Crystallography* **1980**, *13*, 34.

(30) Hamley, I. W.; Stanford, J. L.; Wilkinson, A. N.; Elwell, M. J.; Ryan, A. J. *Polymer* **2000**, *41*, 2569.

(31) Porod, G. *Colloid & Polymer Science* **1951**, *124*, 83.

(32) Porod, G. *Colloid & Polymer Science* **1952**, *125*, 51.
(33) Porod, G. *Colloid & Polymer Science* **1952**, *125*, 108.
(34) Ruland, W. *Journal of Applied Crystallography* **1971**, *4*, 70.
(35) Vonk, C. G. *Journal of Applied Crystallography* **1973**, *6*, 81.
(36) Maeda, M.; Miyasaka, K.; Ishikawa, K. *Journal of Polymer Science Part A-2: Polymer Physics* **1970**, *8*, 355.
(37) Schneider, N. S.; Desper, C. R.; Illinger, J. L.; King, A. O.; Barr, D. *Journal of Macromolecular Science, Part B* **1975**, *11*, 527.
(38) Shen, M.; Mehra, U.; Niinomi, M.; Koberstein, J. T.; Cooper, S. L. *Journal of Applied Physics* **1974**, *45*, 4182.
(39) Van Bogart, J. W. C.; Bluemke, D. A.; Cooper, S. L. *Polymer* **1981**, *22*, 1428.
(40) Koberstein, J. T.; Stein, R. S. *Journal of Polymer Science: Polymer Physics Edition* **1983**, *21*, 1439.
(41) Leung, L. M.; Koberstein, J. T. *Journal of Polymer Science: Polymer Physics Edition* **1985**, *23*, 1883.
(42) Menard, K. P. In *Encyclopedia of Polymer Science and Technology*; John Wiley & Sons, Inc.: 2002.
(43) Pigott, K. A.; Frye, B. F.; Allen, K. R.; Steingiser, S. S.; Darr, W. C.; Saunders, J. H.; Hardy, E. E. *Journal of Chemical & Engineering Data* **1960**, *5*, 391.
(44) Cooper, S. L.; Tobolsky, A. V. *Journal of Applied Polymer Science* **1966**, *10*, 1837.
(45) Wang, C. B.; Cooper, S. L. *Macromolecules* **1983**, *16*, 775.
(46) Huh, D. S.; Cooper, S. L. *Polymer Engineering & Science* **1971**, *11*, 369.
(47) Dickinson, R. B.; Nagel, J. A.; Proctor, R. A.; Cooper, S. L. *Journal of Biomedical Materials Research* **1997**, *36*, 152.
(48) Jeong, E. H.; Yang, J.; Youk, J. H. *Materials Letters* **2007**, *61*, 3991.
(49) Dieterich, D.; Keberle, W.; Witt, H. *Angewandte Chemie International Edition in English* **1970**, *9*, 40.
(50) Petrović, Z. S.; Ferguson, J. *Progress in Polymer Science* **1991**, *16*, 695.
(51) Chattopadhyay, D. K.; Raju, K. V. S. N. *Progress in Polymer Science* **2007**, *32*, 352.
(52) Hwang, K. K. S.; Yang, C.-Z.; Cooper, S. L. *Polymer Engineering & Science* **1981**, *21*, 1027.
(53) Register, R. A.; Pruckmayr, G.; Cooper, S. L. *Macromolecules* **1990**, *23*, 3023.
(54) Register, R. A.; Yu, X.-h.; Cooper, S. L. *Polymer Bulletin* **1989**, *22*, 565.
(55) Ding, Y. S.; Register, R. A.; Yang, C.-z.; Cooper, S. L. *Polymer* **1989**, *30*, 1204.
(56) Yang, C.-Z.; Grasel, T. G.; Bell, J. L.; Register, R. A.; Cooper, S. L. *Journal of Polymer Science Part B: Polymer Physics* **1991**, *29*, 581.
(57) Lee, J. C.; Kim, B. K. *Journal of Polymer Science Part A: Polymer Chemistry* **1994**, *32*, 1983.
(58) Yang, C. Z.; Li, C.; Cooper, S. L. *Journal of Polymer Science Part B: Polymer Physics* **1991**, *29*, 75.
(59) Chen, S.-A.; Hsu, J.-S. *Polymer* **1993**, *34*, 2769.
(60) Santerre, J. P.; Brash, J. L. *Industrial & Engineering Chemistry Research* **1997**, *36*, 1352.
(61) Wei, X.; Yu, X. *Journal of Polymer Science Part B: Polymer Physics* **1997**, *35*, 225.
(62) Szymczyk, A.; Roslaniec, Z. *Polymers for Advanced Technologies* **1999**, *10*, 579.
(63) Szymczyk, A.; Ezquerra, T. A.; Roslaniec, Z. *Journal of Macromolecular Science, Part B* **2001**, *40*, 669.

(64) Szymczyk, A.; Baltá Calleja, F. J.; Roslaniec, Z.; Wlochowicz, A.; Slusarczyk, C. *Journal of Macromolecular Science, Part B* **2002**, *41*, 507.
(65) Phillips, R. A.; Cooper, S. L. *Polymer* **1994**, *35*, 4146.
(66) Phillips, R. A.; Cooper, S. L. *Macromolecules* **1995**, *28*, 5734.
(67) Phillips, R. A.; Cooper, S. L. *Journal of Polymer Science Part B: Polymer Physics* **1996**, *34*, 737.
(68) Phillips, R. A.; McKenna, J. M.; Cooper, S. L. *Journal of Polymer Science Part B: Polymer Physics* **1994**, *32*, 791.
(69) Stevenson, J. C.; Cooper, S. L. *Journal of Polymer Science Part B: Polymer Physics* **1988**, *26*, 953.
(70) Leung, L. M.; Koberstein, J. T. *Macromolecules* **1986**, *19*, 706.
(71) Etienne, S.; Vigier, G.; Cuvé, L.; Pascault, J. P. *Polymer* **1994**, *35*, 2737.
(72) Li, Y.; Gao, T.; Liu, J.; Linliu, K.; Desper, C. R.; Chu, B. *Macromolecules* **1992**, *25*, 7365.
(73) Ophir Zohar, H.; Wilkes Garth, L. In *Multiphase Polymers*; AMERICAN CHEMICAL SOCIETY: 1979; Vol. 176, p 53.
(74) Sheth, J. P.; Aneja, A.; Wilkes, G. L.; Yilgor, E.; Atilla, G. E.; Yilgor, I.; Beyer, F. L. *Polymer* **2004**, *45*, 6919.
(75) Wilkes, G. L.; Abouzahr, S. *Macromolecules* **1981**, *14*, 456.
(76) Wilkes, G. L.; Dziemianowicz, T. S.; Ophir, Z. H.; Artz, E.; Wildnauer, R. *Journal of Biomedical Materials Research* **1979**, *13*, 189.
(77) Wilkes, G. L.; Emerson, J. A. *Journal of Applied Physics* **1976**, *47*, 4261.
(78) Wilkes, G. L.; Wildnauer, R. *Journal of Applied Physics* **1975**, *46*, 4148.
(79) Yilgor, I.; Yilgor, E.; Das, S.; Wilkes, G. L. *Journal of Polymer Science Part B: Polymer Physics* **2009**, *47*, 471.
(80) Velankar, S.; Cooper, S. L. *Macromolecules* **1998**, *31*, 9181.
(81) Velankar, S.; Cooper, S. L. *Macromolecules* **1999**, *33*, 382.
(82) Velankar, S.; Cooper, S. L. *Macromolecules* **2000**, *33*, 395.
(83) Ryan, A. J.; Macosko, C. W.; Bras, W. *Macromolecules* **1992**, *25*, 6277.
(84) Zhang M.; Moore, R. B.; Long, T. E.; *Journal of Polymer Science Part A: Polymer Chemistry*, **In Press**.
(85) Poirier, Y.; Dennis, D. E.; Klomparens, K.; Somerville, C. *Science* **1992**, *256*, 520.
(86) Martina, M.; Hutmacher, D. W. *Polymer International* **2007**, *56*, 145.
(87) Fenouillot, F.; Rousseau, A.; Colomines, G.; Saint-Loup, R.; Pascault, J. P. *Progress in Polymer Science* **2010**, *35*, 578.
(88) Wang, C. S.; Lin, C. H. *Polymer* **2000**, *41*, 4029.
(89) Fox, J. T. G.; Flory, P. J. *Journal of Applied Physics* **1950**, *21*, 581.
(90) Wunderlich, B. *The Journal of Chemical Physics* **1958**, *29*, 1395.
(91) Schawe, J. E. K.; Höhne, G. W. H. *Journal of Thermal Analysis and Calorimetry* **1996**, *46*, 893.
(92) Mano, J. F.; Wang, Y.; Viana, J. C.; Denchev, Z.; Oliveira, M. J. *Macromolecular Materials and Engineering* **2004**, *289*, 910.
(93) Kusy, R. P. *Journal of Polymer Science: Polymer Chemistry Edition* **1976**, *14*, 1527.
(94) Brunette, C. M.; Hsu, S. L.; Rossman, M.; MacKnight, W. J.; Schneider, N. S. *Polymer Engineering & Science* **1981**, *21*, 668.

(95) Koberstein, J. T.; Stein, R. S. *Journal of Polymer Science: Polymer Physics Edition* **1983**, *21*, 2181.
(96) Park, M. J.; Char, K.; Bang, J.; Lodge, T. P. *Macromolecules* **2005**, *38*, 2449.
(97) Minakov, A. A.; Mordvintsev, D. A.; Tol, R.; Schick, C. *Thermochimica Acta* **2006**, *442*, 25.
(98) Marx, C. L.; Caulfield, D. F.; Cooper, S. L. *Macromolecules* **1973**, *6*, 344.
(99) Longworth, R.; Vaughan, D. J. *Nature* **1968**, *218*, 85.
(100) Eisenberg, A.; Hird, B.; Moore, R. B. *Macromolecules* **1990**, *23*, 4098.
(101) Mauritz, K. A.; Moore, R. B. *Chemical Reviews* **2004**, *104*, 4535.
(102) Grasel, T. G.; Cooper, S. L. *Journal of Biomedical Materials Research* **1989**, *23*, 311.
(103) Buruiana, E. C.; Buruiana, T. *Journal of Photochemistry and Photobiology A: Chemistry* **2002**, *151*, 237.
(104) Verma, R. K.; Velikov, V.; Kander, R. G.; Marand, H.; Chu, B.; Hsiao, B. S. *Polymer* **1996**, *37*, 5357.
(105) Storey, R. F.; Baugh, D. W. *Polymer* **2001**, *42*, 2321.